Absorption Spectroscopy in High-Finesse Cavities for Atmospheric Studies

Steven S. Brown

NOAA Aeronomy Lab, R/AL2, 325 Broadway, Boulder, Colorado 80305, and Cooperative Institute for Research in the Environmental Sciences, University of Colorado, Boulder, Colorado 80309

Received March 6, 2003

Contents

1. Introduction 5219
2. Cavity Ring-Down Spectroscopy (CRDS) 5221
   2.1. Pulsed CRDS 5223
   2.2. Broad-band CRDS 5223
   2.3. Continuous-Wave (CW) CRDS 5223
3. Cavity-Enhanced Absorption (CEA) and Integrated Cavity Output Spectroscopy (ICOS) 5224
4. Spectral Regions 5225
5. Atmospheric Trace Gas Detectors 5225
   5.1. Methane, Hydrocarbons, and Formaldehyde 5227
      5.1.1. Methane 5227
      5.1.2. Hydrocarbons 5227
      5.1.3. Formaldehyde 5229
   5.2. Carbon Monoxide and Carbon Dioxide 5229
   5.3. Ammonia 5230
   5.4. Nitrogen Oxides 5230
      5.4.1. NO and NO_2 5230
      5.4.2. NO_3 and N_2O_5 5232
      5.4.3. HONO 5233
   5.5. Hydroxyl Radical 5233
   5.6. Elemental Mercury 5233
   5.7. Isotope Ratios 5234
6. Aerosol Extinction 5235
7. Conclusion 5237
8. Acknowledgments 5237
9. References 5237

Steven S. Brown received his Bachelor's degree in Chemistry at Dartmouth College in 1989 and his Ph.D. degree in Physical Chemistry from the University of Wisconsin—Madison in 1996. He came to the NOAA Aeronomy Lab in 1997 as a National Research Council postdoctoral fellow. In 2000 he joined the permanent staff of the Aeronomy Lab as a research scientist with the Cooperative Institute for Research in the Environmental Sciences at the University of Colorado, Boulder, a joint institute with NOAA. His research efforts at NOAA have focused on the atmospheric chemistry of nitrogen oxides, most recently in field measurements of the nocturnal compounds NO_3 and N_2O_5.

1. Introduction

Much of the important chemistry of the atmosphere takes place on exceedingly small concentration scales, with principle components occurring at mixing ratios that vary from the part per million by volume (ppmv) level (e.g., CO, CO_2) to scales smaller than a part per trillion (pptv) (e.g., OH radical). Characterizing the abundance of trace compounds is of the utmost importance in developing a chemical picture of the atmosphere; as a result, sensitive trace gas detection is fundamental to atmospheric science. Many extremely specific and sensitive techniques are currently in practice, from mass spectrometry and gas chromatography to optical methods such as laser-induced fluorescence, chemiluminescence, and direct absorption. One important advantage to the latter is that it is an absolute concentration measurement presuming the absorption cross section of the target species is known; among its disadvantages is the path length required to achieve sufficient sensitivity for detection of trace species at their atmospheric concentration levels. For example, many trace compounds with strong, structured ultraviolet and visible absorption bands have been characterized by observation of their characteristic spectra on kilometer-scale open paths in the atmosphere via differential optical absorption spectroscopy (DOAS). Recent advances in absorption spectroscopy, including, for example, frequency and wavelength modulation techniques in tunable diode laser spectroscopy, and photoacoustic spectroscopy have significantly improved the sensitivity of absorption measurements and have made in-situ atmospheric detectors based on direct absorption feasible. In gaining sensitivity, however, these techniques in many cases sacrifice the absolute concentration determination inherent to other direct absorption methods.[1,2]

The application of high-finesse optical cavities (i.e., stable optical resonators with high reflectivity mirrors) to sensitive absorption measurements began in earnest a decade and a half ago with the development of cavity ring-down spectroscopy (CRDS).[3] This technique is now well established and has seen application to a wide variety of environments, from plasmas and flames to supersonic expansions.[4−7] A more

10.1021/cr020645c CCC: $44.00
Published on Web 11/07/2003

recent development is high-sensitivity absorption measurements based on the integrated intensity passing through a high-finesse cavity, alternatively called cavity-enhanced absorption (CEA)[8] or integrated cavity output spectroscopy (ICOS).[9,10] The discussion below refers to the two techniques collectively as "high-finesse cavity absorption spectroscopy" or HFCAS. Although this review considers both CRDS and CEA/ICOS, the emphasis is on CRDS since it is more thoroughly developed.

One of the recent trends in HFCAS has been its application in instruments designed as sensors for trace gases in the atmosphere. Interestingly, the first CRDS-based studies published after its introduction in 1988 concerned near-infrared spectroscopy of water vapor in an open path of air[11] and detection of ambient NO_2.[12] Through the decade of the 1990s, a period during which the number of CRDS-based studies accelerated remarkably,[13] the subject of trace species detection in ambient air via CRDS was the main topic of only a handful of publications.[14−16] The first few years of the current decade, however, have witnessed dozens of publications on the subject, and many more are surely in preparation even at the time of this writing. Many of the new publications are "proof of concept" papers, outlining potential applications with only brief demonstrations of (or in some cases just inferences about) real-world performance. Examples of HFCAS measurements with geophysical interpretation remain scarce. Given the number of researchers now involved and the variety of systems to which CRDS CEA/ICOS measurements are applicable, we may expect atmospheric trace species detection via these methods to be a true growth industry over the next several years.

As a method for detection of trace species in the ambient atmosphere, HFCAS holds a great deal of promise. The potential advantages are severalfold. The first is its sensitivity, which approaches (although it is not generally equal to) that of fluorescence or mass spectrometry, both of which are (at least in principle) dark background methods.[7] The second is the absolute nature of CRDS measurements, which requires no calibration provided that the absorption cross section is known and the inlet and sampling losses are well characterized. (A description of CEA ICOS calibrations appears below.) Like other spectroscopic methods that take advantage of the inherently high resolution of laser light sources, HFCAS can be highly specific to the particular species of interest. It is also an in situ method with a rapid response time, allowing for high spatial and temporal resolution in atmospheric measurements. Depending on the particular experimental approach (see below), HFCAS instruments can be simple, robust, compact, lightweight, and low in power consumption. These attributes make them versatile for deployment on a variety of platforms, including ships, aircraft, etc. Finally, HFCAS is applicable not just to measurements of homogeneous, gas-phase absorption, but to scattering and absorption due to atmospheric particulate matter. The latter is a particularly powerful new application for atmospheric measurements.

That said, HFCAS is not without its down sides for atmospheric sampling. Its extreme sensitivity to aerosol extinction in the ultraviolet, visible, and near-infrared leads to difficulties in gas-phase detection if an inlet filter is not used, making it potentially impractical for sampling reactive compounds. Like any in-situ method, sampling issues and inlet losses are an important concern. As we will see below, there are numerous experimental variations on HFCAS dictated mainly by the coupling between laser sources and optical cavities. While some approaches are simple, others are not, and the very highest sensitivities are in many cases associated with the more complex experimental arrangements. Particular laser sources that may be ideal for the detection of particular compounds may not allow for easy construction of a field-ready HFCAS-based detector. Finally, there are already many highly sensitive, mature technologies that have been developed for detection of specific trace gases. Since HFCAS techniques are relatively novel, they may prove to be competitive for certain compounds and not for others. Where possible, this review compares the currently available detection sensitivity and sampling issues for specific compounds with either the demonstrated or projected sensitivity of HFCAS. Since most of these instruments are prototypes, many do not compare favorably with existing schemes that have been through several stages of instrument development. Nevertheless, one would anticipate that the inherent sensitivity of the technique will make it applicable to a wide range of trace species in the future.

The scope and outline of this review is as follows. It begins with a description of the principle behind CRDS and related spectroscopies (now familiar to many readers) and discusses a few of the relevant experimental approaches. It then goes on to describe currently published reports on HFCAS instruments that have been developed or are under development for atmospheric trace gas detection. The criterion for inclusion of any particular study is that one of its principle goals be for the design of an instrument (even a laboratory based prototype) useful for sampling and quantification of an atmospherically relevant trace compound from ambient air. Studies demonstrating measurements of atmospherically important compounds, but for other purposes, such as spectroscopic or combustion studies, have been excluded. For example, numerous authors have recorded spectra of water vapor or molecular oxygen, in some cases in ambient air samples, but not for the purpose of ascertaining their atmospheric concentrations. The common theme that ties all of the reviewed studies together is the use of high-finesse optical cavities for concentration measurements of trace species in ambient air.

After the preparation of this manuscript, a review appeared by Atkinson[17] outlining the application of CRDS for a variety of problems important to environmental chemistry. The Atkinson review is somewhat different in scope and emphasis than the present one, though it necessarily covers much of the same literature. The two reviews are useful complements, and the reader is encouraged to refer to both.

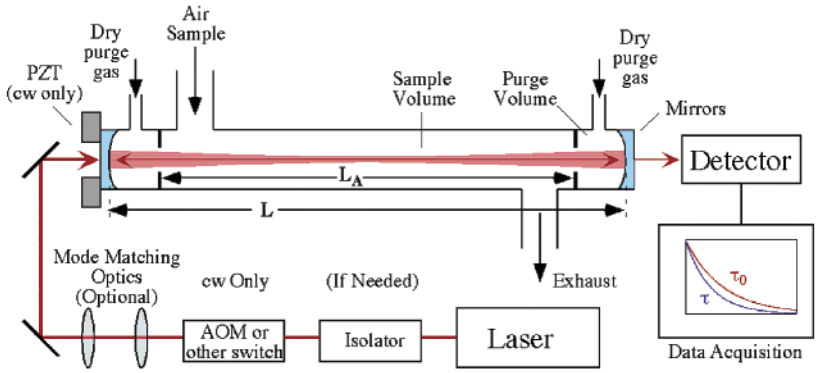

Figure 1. Generalized schematic of a cavity ring-down spectrometer.

2. Cavity Ring-Down Spectroscopy (CRDS)

The following discussion is necessary for completeness. Its general features have, however, appeared in several previous publications on the subject of cavity ring-down spectroscopy and may be quite familiar to many readers. The reader may refer to a number of excellent recent reviews on the subject of cavity ring-down spectroscopy itself.[4−7] Further consideration of CEA and ICOS methods appear in the next section, although the following general description of the properties of high-finesse optical cavities applies to both CRDS and CEA/ICOS.

Conventional spectroscopy is based on the measurement of the change in the intensity, I, of light as it passes through an absorbing medium (i.e., the Beer−Lambert law). The most important limiting factors to the sensitivity are the path length through the medium and the measurement of a small intensity change in a bright, potentially noisy, light source. There are several schemes that improve the available path length, such as multipass configurations (i.e., White or Herriot cell optics) or, specifically for atmospheric measurements, long open paths. Modulation schemes are useful for extracting a signal from a small intensity change over the bandwidth of a narrow absorption line.

Cavity ring-down spectroscopy circumvents the path-length constraints of conventional spectroscopy by taking advantage of the properties of high-finesse optical cavities, which trap photons for finite periods of time. Rather than an intensity change, CRDS measures the time decay of light intensity from an optical cavity. A CRDS measurement consists of three steps: introduction of a light source into the optical cavity, a rapid switch of the intensity away from the cavity, and observation of the intensity decay from the cavity. Figure 1 shows a general schematic for a two-mirror cavity. If the only loss from the cavity is due to the finite transmission through the mirrors, it is straightforward to show that the intensity decays as a single exponential. If, on the other hand, there is an absorber (or scatterer) present within the cavity, the combination of mirror transmission losses and the absorption loss due to Beer's law will also give rise to a single-exponential decay but with a faster time constant. A measurement of the characteristic decay time constants in the presence and absence of the absorber yields its concentration, [A], directly for known absorption cross section, σ.

$$\alpha = [A]\sigma = \frac{R_L}{c}\left(\frac{1}{\tau} - \frac{1}{\tau_0}\right) \quad (1)$$

Here, α is the absorption coefficient (cm^{-1}) for the target compound, $1/\tau_0$ and $1/\tau$ are the first-order decay rate constants from the empty cavity and the cavity containing the absorber, respectively, c is the speed of light, and R_L is the ratio of the cavity length, L, to the length over which the absorber is present, L_A (see Figure 1). The factor R_L can be important for CRDS measurements in the atmosphere because of the necessity in some applications to maintain the cleanliness of the mirrors even while the sample contains condensable gases and aerosol; one simple solution to this constraint, shown in Figure 1, is a volume adjacent to each mirror that is purged by clean, dry gas.

The actual value of τ_0 in eq 1 for atmospheric sampling is due to the sum of several loss processes that include mirror transmission, Rayleigh scattering, Mie scattering, and interferences from absorbers other than the target species.

$$\frac{1}{\tau_0} = c\left(\frac{T}{L} + \alpha_{\text{Rayleigh}} + \frac{\alpha_{\text{Mie}}}{R_L} + \frac{1}{R_L}\sum_i \alpha_i\right) \quad (2)$$

Here, α_{Rayleigh} and α_{Mie} are the absorption coefficients (cm^{-1}) for Rayleigh and Mie scattering, and α_i are the absorption coefficients for any gas-phase species other than the target compound. The factor T is the mirror transmission, assumed for simplicity to be $T = 1 - R$, where R is the reflectivity. If there are other loss processes in the mirror itself, such as scattering or absorption within the dielectric coatings, the value of T represents the sum of all mirror losses. Equation 2 assumes that purge volumes in Figure 1 are filled with pure, particulate-free buffer gas of the same refractive index as the air in the sample volume. From a practical standpoint, detailed knowledge of the contributions of the individual terms in eq 2 is unimportant. One needs only to know the value of τ_0 and its reproducibility.

The sensitivity of CRDS comes largely from the path length in the high-finesse cavity. For mirrors of suitably large reflectivity (the state of the art is roughly $R = 0.99999$ or $T = 10$ parts per million, ppm, in the visible and near-IR) and moderately long

cavities (1 m, for example), the τ_0 value in eq 1 could in theory exceed 300 μs, corresponding to a path length of roughly 100 km in a single (1/e) lifetime. Although more typical instruments have τ_0 values that fall in the range 1−100 μs, the available path length can easily exceed that which is possible even with long open path spectroscopy. An additional sensitivity advantage to CRDS for the case of particularly noisy light sources (e.g., pulsed dye lasers with pulse to pulse energy fluctuations of several percent) is that the rate constant for the intensity decay from the optical cavity is independent of the intensity itself. Thus, as long as the actual intensity decay closely follows a single exponential, fluctuations in the light source do not add to the noise level of the measurement.

Taking the limit of eq 1 in which τ approaches τ_0, one arrives at an expression for the sensitivity of a CRDS measurement.[18]

$$\alpha = \frac{R_L}{c}\left(\frac{1}{\tau} - \frac{1}{\tau_0}\right) = \frac{R_L}{c}\left(\frac{\tau_0 - \tau}{\tau \cdot \tau_0}\right) \approx \frac{R_L}{c}\frac{\Delta\tau_0}{{\tau_0}^2} \text{ as } \tau \rightarrow \tau_0 \quad (3)$$

Here $\Delta\tau_{min}$ is the smallest measurable difference between τ and τ_0 and can most conveniently be taken as an integral number (i.e., 1, 2, or 3) of standard deviations in τ_0. Taking the quantity $\delta\tau_0$ as the fractional uncertainty in τ_0 (i.e., $\Delta\tau_0/\tau_0$), eq 4 gives the minimum detectable absorption coefficient, α_{min}.

$$\alpha_{min} = \frac{R_L}{c}\frac{\delta\tau_0}{\tau_0} \quad (4)$$

The value of α_{min} is often expressed as cm^{-1} $Hz^{-1/2}$ in order to account for the integration time required to achieve a particular sensitivity. One may improve the sensitivity of a CRDS measurement in three ways. The first is to improve the reproducibility of the intensity decays from the optical cavity to minimize $\delta\tau_0$. The second is to increase the cavity length or mirror reflectivity to maximize τ_0. (Changing the mirror reflectivity will change the finesse of the cavity and so influence the coupling to the laser source, see below.) Finally, increasing the repetition rate with which ring-down transients are acquired to maximize the duty cycle of the measurement improves either the sampling rate or increases the sample averaging in a given integration period. The following discussion will consider sensitivities of different experimental approaches and of individual instruments with respect to each of these factors. The values for α_{min} reported to date vary widely depending on the details of the experimental arrangement, from 10^{-12} to 10^{-6} cm^{-1} $Hz^{-1/2}$. The lower end of this range is easily sufficient to detect ambient levels of a host of trace gases in the atmosphere, although it has not been realized in field-ready prototype instruments to date.

The foregoing discussion has considered only the extraction of a concentration from a CRDS measurement without regard for the means by which the light source was introduced into the optical cavity. The discussion of experimental CRDS schemes depends most importantly on the behavior of light in a high-finesse optical cavity, and so a brief introduction to this topic is helpful at this point. A more detailed discussion appears in Busch and Busch[4] and in many standard optics texts. The reflectivity of the mirrors determines the "finesse", F, of the cavity as $F = \pi\sqrt{R}(1 - R)$. In the CW limit, a high-finesse optical cavity, or Fabry−Perot resonator, transmits light at a series of discrete frequencies determined by the condition of constructive interference on successive passes. Figure 2 illustrates this phenomenon for a relatively short (25 cm), two-mirror cavity with low-reflectivity mirrors ($R = 0.9$). The spacing between successive fundamental modes, or free spectral range (FSR, given below in units of Hz), is inversely proportional to the cavity round trip length.

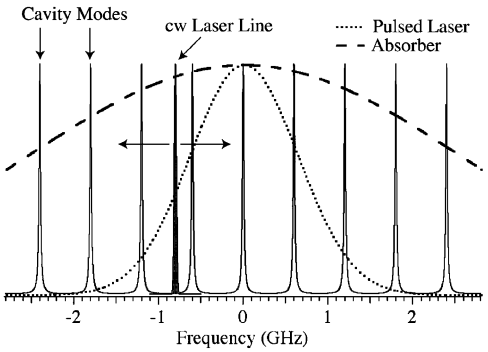

Figure 2. Illustration of overlap between the modes of an optical cavity, the lines of CW and pulsed laser sources, and the line width of an arbitrarily chosen absorber. The cavity modes have been arbitrarily spread out and broadened by choosing a length of 25 cm, a mirror reflectivity of 90%, and displaying only the longitudinal (TEM_{00}) modes. The spectrum of modes in an actual cavity will be considerably more dense. The pulsed laser line width is chosen at 1.5 GHz (0.05 cm^{-1}) fwhm, while the CW line width has been arbitrarily set to 30 MHz (0.001 cm^{-1}) in order to make its width visible in the figure. Actual widths of cavity modes and CW laser lines are likely to be significantly narrower than those depicted here. An arbitrary absorption with a Gaussian line width of 6 GHz (0.2 cm^{-1}) is superimposed as the dashed line. The figure illustrates the passive match to cavity resonances achieved with a pulsed laser source and the need to actively match the frequency of a CW laser to the same mode structure. It also shows the potential pitfall of an absorption line that varies rapidly within the line width of a pulsed laser, an effect that can lead to nonexponential ring-down transients.

$$\text{FSR} = \frac{c}{2Ln\cos\theta} \quad (5)$$

Here L is the cavity length, n the refractive index of the medium, and θ the angle of incidence ($\cos\theta = 1$ for normal incidence, the usual case for CRDS). The fundamental modes are also known as TEM_{00} or zero-order transverse electric modes and also as longitudinal modes. Higher order transverse electric modes have a frequency spectrum that depends on the geometry of the particular resonator but usually fall between successive TEM_{00} frequencies (not show in Figure 2). The full widths (fwhm) of the cavity resonances depend on the free spectral range and on the reflectivity or the mirrors.

$$\text{fwhm} = \frac{\text{FSR}}{\pi}\left(\frac{1 - R}{\sqrt{R}}\right) \quad (6)$$

For mirrors of very high reflectivity (e.g., 0.99999), the resonances become extremely narrow (on the order of kHz for cavities of tens of centimeters) in the CW limit.

The following section briefly outlines a few of the different experimental approaches to cavity ring-down measurements. A more detailed review can be found in Berden et al.[7]

2.1. Pulsed CRDS

The original concept of cavity-ring down spectroscopy[3] was the introduction of a short (i.e., nanosecond time scale) laser pulse into an optical cavity followed by observation of the resulting intensity decay. This method is now often referred to as "conventional" cavity ring-down. It remains the most experimentally straightforward means of coupling laser light into a cavity. Nanosecond scale laser pulses are rapid relative to the intensity decay from a high-finesse cavity, so that switching the light source away from the cavity after excitation occurs automatically. The most important simplifying factor, however, is the facile coupling of pulsed lasers to optical cavities because of their broad line widths (e.g., tunable dye lasers, with $\Delta\nu \geq 1$ GHz), which is typically broader than the free spectral range. It consequently overlaps spectrally with a number of resonances regardless of the center frequency of the laser pulse. Figure 2 illustrates this phenomenon. The laser simply fills up all modes (TEM_{00} or higher) to which it may couple spatially and that lie underneath its frequency envelope. Additionally, the introduction of a pulsed light source into the cavity has the effect of broadening the widths of individual resonances, especially as the pulse duration of the external laser source becomes equal to or less than the round trip time.[19]

As long as each individual resonance coupled to the laser decays with the same, or at least approximately the same, decay rate and as long as interference effects between higher order transverse electric modes at different frequencies are not severe, ring-down transients from pulsed excitation of an optical cavity are single exponentials and eq 1 is valid. However, each of these effects may lead to nonexponentially decaying ring-down transients that complicate the extraction of a single, well-defined time constant. This topic has been considered by several authors in some detail[20−24] and is beyond the scope of this review. For the current discussion, it is sufficient to say that single-exponential behavior in pulsed CRDS is common and relatively easy to achieve. The advantage to a pulsed CRDS instrument is its simplicity. Very little is required other than a laser source, turning and focusing optics, an isolator if one is necessary, cavity mirrors, and a detector. The alignment tends to be robust and insensitive to vibrations, even in field environments and on mobile platforms such as ships.

There are, however, several important disadvantages to the pulsed variety of CRDS. The broad spectral bandwidth of pulsed lasers is often inappropriate for detection of small molecules via discrete rovibrational transitions with narrow line widths. Again, Figure 2 illustrates this point. If the absorption cross section of the target compound varies significantly over the bandwidth of the light within the cavity, different frequencies of laser light experience different decay rates and the overall intensity decay becomes multiexponential. While there are methods for dealing with this difficulty, particularly for the weak absorption signals likely to arise from atmospheric trace gas detection, it is a complicating factor for pulsed CRDS absorption measurements.[19,25−27] Consequently, pulsed CRDS is more appropriate for compounds with relatively broad bandwidth transitions, including electronic transitions in the visible or ultraviolet (e.g., NO_3, NO_2, halogen oxides, etc.) or the congested spectra of overlapping rovibrational bands characteristic of larger molecules (e.g., HNO_3[28]). Additionally, pulsed lasers often have slow repetition rates (e.g., commercial Nd:YAG lasers that operate at 10−100 Hz) that limit the acquisition rate for ring-down transients. Also, the spectral scanning process for many tunable pulsed lasers (e.g., dye lasers, OPOs) is rather time consuming since it usually involves movement of mechanical parts rather than ramping of a temperature or a current as in a diode laser. Finally, although smaller-footprint, lower-power pulsed laser sources are becoming more common, pulsed laser sources are still often relatively bulky and may have appreciable power requirements, making them less desirable in the design of field instruments.

2.2. Broad-band CRDS

A variation on pulsed CRDS that exploits the inherently broad-band nature of some pulsed lasers is the dispersion of a broad-band, pulsed light source *after* it exits an optical cavity.[29] Alternatively called ring-down spectral photography,[30,31] ring-down spectrography,[32] or Fourier transform cavity ring-down spectroscopy,[33] a review of this method by Ball and Jones appears in this issue.

2.3. Continuous-Wave (CW) CRDS

Continuous-wave CRDS seems, on the surface, to be a contradiction in terms, since "ring-down" is an inherently time-dependent method. However, Romanini et al.[34,35] and Paldus et al.[36] showed in 1997 that the combination of a CW laser-pumped optical cavity and a fast optical switch could be used to make high-sensitivity measurements. A narrow-band CW laser source, whose frequency is matched to that of a single cavity resonance, builds power into the selected mode. Rapid switching of the intensity away from the cavity using, for example, an acousto-optic modulator (AOM), allows for observation of a ring-down transient in the same fashion as described above. Because CW laser sources are generally quite narrow in comparison to pulsed laser sources—typically much narrower than the free spectral range of the cavity—the condition of resonance between the laser frequency and cavity resonance is not automatic. Figure 2 shows a CW laser line (with an arbitrarily large line width for clarity of presentation) whose frequency lies between the cavity resonances.

The advantage to CW CRDS is the excitation of a single, well-characterized cavity mode with the ensuing reproducibility of ring-down transients and the lack of interference effects between modes of different frequencies.

There are any number of techniques for matching the frequency of a CW laser to that of an optical cavity. The "standard" method, and the one used in many of the applications described below, was introduced by Romanini et al.[34] A piezoelectric transducer (PZT), to which one of the cavity mirrors is mounted, sweeps the frequency of the cavity resonance spectrum through at least one free spectral range at a fixed laser frequency. Light builds into the cavity whenever a resonance occurs, and a threshold circuit triggers the fast switch to record a ring-down decay only when there is sufficient intensity at the detector. He and Orr[37] reported a variation on this approach in which the cavity sweep is fast compared to the ring-down time constant, such that it sweeps itself out of resonance and removes the need for a fast switch. An analogous, but less commonly used method, is to sweep the laser frequency repeatedly through one free spectral range at a fixed cavity length.[38]

These approaches depend on accidental matches during a frequency scan and do not result in optimum buildup of laser power into the cavity. Actively locking the laser frequency to a cavity resonance (e.g., Pound−Drever−Hall method) allows for the best coupling between the laser and cavity and thus the largest power buildup.[39] This can result in a higher repetition rate for acquisition of ring-down transients and in improved signal-to-noise for individual ring-down events. It is, however, experimentally more complicated and remains untested in a field environment, although the potential sensitivity gain is impressive. For example, Spence et al.[40] demonstrated a CRDS scheme with an active lock between the frequency of a diode pumped, CW Nd:YAG laser (1.06 μm) and a three-mirror cavity that had a repetition rate greater than 80 kHz and a sensitivity of $\alpha_{min} = 10^{-12}$ cm^{-1} Hz$^{-1/2}$ (short-term stability) or 9 $\times$ 10^{-12} cm^{-1} Hz$^{-1/2}$ (long-term stability). Likewise, combination of CRDS with optical heterodyne detection,[41] in which the beam exiting the cavity overlaps with a second laser beam of a slightly different frequency and the beat frequency between the two is observed, can also lead to large sensitivity increases.

The CW variant of CRDS does not suffer from the laser bandwidth constraint of pulsed CRDS and is consequently the most widely applicable method for atmospheric trace gas detection. Rapid scanning over single lines with CW laser sources is possible if spectral discrimination between on- and off-resonance signals is required for zero measurements. The matching between cavity and laser frequencies and the subsequent intensity switching can occur at high repetition rates, allowing for faster acquisition of ring-down transients (i.e., greater signal averaging) than is possible with fixed repetition rate pulsed lasers. Many CW laser sources are compact and have low power consumption (e.g., diode lasers), making them easy to integrate into a portable instrument. The disadvantages to the CW CRDS approach, aside from the reduction in experimental simplicity, include the limited availability of laser sources in some spectral regions (see below) and the narrow range of frequency tunability for many CW sources, which makes them less optimal for detection of species with broad features in their absorption spectra. Saturation of an absorption line is also more likely to occur in CW CRDS,[18] particularly if there is an active lock between the laser and the cavity.

3. Cavity-Enhanced Absorption (CEA) and Integrated Cavity Output Spectroscopy (ICOS)

Absorption spectroscopy in high-finesse cavities is not restricted to the time-domain measurements of CRDS alone. Several recent demonstrations have shown that the integrated intensity passing through an optical cavity can serve as an equally sensitive absorption measurement. These schemes, called either cavity-enhanced absorption (CEA)[8] or integrated cavity output spectroscopy (ICOS),[9,10] are applicable to either pulsed or CW laser pumping of an optical cavity, although the CW approach has seen much more frequent use in this rapidly developing field. The approach involves several steps. The first is the intentional mode matching of the input laser to many different cavity modes (i.e., TEM_{00} and higher order) and the choice of a resonator geometry with a mode spectrum that is spread out in frequency. The second is to record a series of laser frequency scans through this mode spectrum, where the scan rate is rapid enough to suppress interference effects at any given frequency. Finally, dithering one of the cavity end mirror positions shifts the mode spectrum on successive laser scans. The average of many such scans shows a transmission through the cavity that is independent of frequency.

Unlike CRDS, the CEA/ICOS scheme does not provide a stand-alone absolute intensity measurement. To extract absolute absorptions, the cavity loss in the absence of the absorber, conveniently expressed as the ratio of the mirror transmission, T, to the cavity length, L, must be known. Equation 7 below gives the absorption coefficient at a given laser frequency as a function of the intensity in the presence (I) and absence (I_0) of an absorber.[7]

$$\alpha = \frac{T}{L} \times \left(\frac{I_0}{I} - 1 \right) \tag{7}$$

A standard time-domain ring-down measurement serves as a convenient calibration for the cavity loss. Although the CEA/ICOS approach is relatively simple, quantitative analysis requires the tandem use of this approach with CRDS or an equivalent calibration.

A promising, recent variation on this scheme reported by Paul et al.[42] is the use of off-axis alignment of the input laser (off-axis integrated cavity output spectroscopy, OAICOS). The alignment is similar to that of an astigmatic Herriot cell, except without input and output holes in the mirrors. Light enters the cavity directly through one end mirror at a point off of the cavity axis and makes a long, folded path that it eventually retraces. The effective cavity

length is many times the base path, with the result that the free spectral range becomes much narrower than that of a cavity with on-axis alignment (see eq 5). As individual cavity modes overlap, the laser frequency is effectively always in resonance with the cavity and the transmission function becomes frequency independent. The off-axis back-reflection of the laser from the front cavity mirror does not feed back into the laser source, removing the need for isolation. The instrument can function either in the time-domain as a ring-down spectrometer or in the integrated intensity domain. The approach, as outlined in the few papers that have appeared to date, has an exceedingly simple (and therefore, presumably robust) experimental design. It has seen only one significant application to atmospheric trace gas detection; however, it proved to have excellent sensitivity for detection of a number of relevant compounds[43] (see below). Tests of this technique from a variety of laboratories are likely to occur soon and will be important in confirming its applicability for atmospheric monitoring.

4. Spectral Regions

There are now demonstrations of HFCAS in spectral regions spanning the entire range from the deep ultraviolet to the mid-infrared[7,44] and also, recently, the millimeter wave region.[45] The limitations are the availability of laser light sources, high-reflectivity mirrors, and sensitive detectors. The properties of the atmosphere itself and the spectral characteristics of different molecules impose some additional constraints on the suitability of different wavelength regions for HFCAS detection of atmospheric trace species. The atmosphere, for example, gives rise to background losses due to both Rayleigh and Mie scattering, as in eq 2. Different classes of compounds have strong, accessible absorption bands in different regions; certain open-shell compounds are amenable to visible and near-ultraviolet detection, while many stable gases are most easily probed via near- and mid-infrared rovibrational bands.

The ultraviolet is a region where many compounds possess strong electronic absorption spectra; it is, however, a difficult region for sensitive HFCAS detection.[44] Although pulsed laser sources that cover the entire UV are readily available (e.g., frequency-doubled dye lasers, fixed frequency Nd:YAG harmonics, and excimer lasers), high-reflectivity UV mirror coatings are not as efficient. Rayleigh and Mie scattering processes have steep wavelength dependences and contribute significantly to the loss from an optical cavity at or near ambient pressure. (Conversely, if one is interested in *measuring* Mie scattering, the UV is the most sensitive region, see below.) These effects combine to limit the maximum possible τ_0 values to tens rather than hundreds of microseconds.[18] Finally, because of the large number of compounds present in the atmosphere with diffuse, overlapping UV bands (particularly O_3), spectroscopic interferences can be severe.

The visible is a convenient region for HFCAS. Laser sources, both pulsed and CW, are available (e.g., pulsed dye lasers, tunable diode lasers) as are mirrors of excellent reflectivity (as low as $T \leq 10$ ppm). Rayleigh scattering drops off across this region and does not impose an appreciable limitation on losses from an optical cavity at ambient pressure at the red end of the visible.[18] Mie scattering remains important but can be controlled by filtering the air sample. Unfortunately, the visible is a largely transparent region for many atmospheric trace species. The exceptions include open-shell compounds with low-lying electronic states (e.g., NO_2 and NO_3). Water vapor also has a strong atmospheric overtone spectrum in the visible due to its abundance. These bands, along with the visible bands of molecular oxygen, can serve as an interference, however, for optical detection of other compounds.

The near-infrared (0.8−3 μm) is a region where overtone and combination band spectra of small, atmospherically relevant molecules (particularly those with an X−H stretch vibration, where X = C, N, O, S, etc.) carry sufficient intensity to allow detection of atmospheric concentrations of some compounds. Rayleigh scattering becomes an unimportant cavity loss at atmospheric pressure in this region. Near-IR laser sources, particularly CW diode lasers, are now readily available and inexpensive. Because rovibrational overtone spectra of small molecules (e.g., methane, CO_2) consist of discrete Doppler and pressure-broadened lines, CW CRDS and CEA/ICOS is more appropriate for atmospheric detection in this region than is pulsed CRDS. A host of near-IR prototype instruments for a variety of purposes and target compounds is currently under development.

The mid-infrared (3−10 μm), or fingerprint region, encompasses fundamental molecular vibrational transitions which are 2 orders of magnitude more intense than first overtones of even highly anharmonic oscillators.[46] Scherer et al.[47] first demonstrated the possibility of CRDS detection in this region by recording the spectrum of CH_4 with a pulsed OPO system. Later, Paldus et al.[48] showed the feasibility of CW mid-IR CRDS using a cryogenically cooled quantum cascade laser to detect ammonia. Unfortunately, the same kind of small, inexpensive, simple laser systems that are common in the near-IR are not available in the mid-IR. Pulsed OPOs can cover a large fraction of this region but have broad line widths. Available, portable mid-IR CW laser systems include Pb salt diode and quantum cascade (QC) lasers, both of which must be liquid nitrogen cooled, and difference frequency generation schemes.[49] Quantum cascade lasers are a promising new technology that may soon offer small-scale, ambient-temperature, high-power, mid-IR CW light sources.

5. Atmospheric Trace Gas Detectors

This section describes existing instruments based on HFCAS for detection of trace gases in the ambient atmosphere. It is arranged according to the general class of compound and includes hydrocarbons, CO, CO_2, ammonia, nitrogen oxides and their acids, OH, and mercury. Also considered is the measurement of isotopic enrichment in the atmosphere. Finally, there is a description of the application of HFCAS to the determination of the optical properties of atmospheric

Table 1. Summary of Quoted Performances of Different Trace Gas and Aerosol Detectors Based on High-Finesse Cavity Absorption

species	ref	method	λ (μm)	sensitivity[a] (cm^{-1})	mixing ratio[b] (ppbv)	int. time[c]	sample
CH_4	53	CW CRDS	1.65	1.5×10^{-8}	52	15 min	lab air
	54	CEA/ICOS	1.73	1.8×10^{-7}	3400	1 s	CH_4/Ar mix
	43	OAICOS	1.65	1×10^{-11}	0.3	1 s	lab air
C_2H_6	57	locked CRDS	3.3	1×10^{-9}	0.1	5 s	human breath
C_2H_4	16	locked CRDS	10.6	3×10^{-8}	1	100 s	C_2H_4/N_2 mix
	59	CEA/ICOS	10.5	1.5×10^{-6}	5	1 s	C_2H_4/N_2 mix
	60	CW CRDS	1.6	1.3×10^{-8}	78	30-90 s	C_2H_4/Ar mix
C_2H_2	61	CW CRDS	1.5	$\sim 4 \times 10^{-9}$	4	2 s	flame
	60	CW CRDS	1.6	1.3×10^{-8}	0.9	30-90 s	C_2H_2/Ar mix
	43	OAICOS	1.5	1×10^{-11}	0.1	1 s	$_{C2}H_2/N_2$ mix
TNT	62	pulsed CRDS	6−8	9×10^{-9}	0.075	1 s	synthetic
chloro-benzenes	15	pulsed CRDS	0.266		ppm levels		lab sample
CH_2O	44	pulsed CRDS	0.32	4×10^{-7}	300		
	68	CEA/ICOS	1.76	1×10^{-8}	350		pure gas
	69	locked CRDS	3.5	7×10^{-9}	2	2 s	cylinder
CO_2	74	rapidly swept CW CRDS	1.5	2.5×10^{-9}		1 s	pure gas
	61	CW CRDS	1.57	$\sim 4 \times 10^{-9}$	2500	2 s	lab air
CO	61	CW CRDS	1.57	$\sim 4 \times 10^{-9}$	2000	2 s	pure gas
	43	OAICOS	1.56	1×10^{-11}	12	1 s	lab air
NH_3	14	pulsed CRDS	0.204		10		NH_3/air mix
	80	CEA/ICOS	1.5	2×10^{-8}	100	1 s	NH_3/air mix
	48	CW CRDS	8.5	4×10^{-9}	0.25	1 s	NH_3/N_2 mix
	61	CW CRDS	1.5	$\sim 4 \times 10^{-9}$	19	2 s	NH_3/N_2 mix
	43	OAICOS	1.5	1×10^{-11}	2	1 s	NH_3/air mix
NO	84	CEA/ICOS	5.2		16		human breath
	49	CW CRDS	5.2	5×10^{-8}	0.7	8s	human breath
	87	pulsed CRDS	0.226		~20000	7 min	engine exhaust
NO_2	12, 85	pulsed CRDS	0.43−0.46		≪16	1 s	lab air
	15	pulsed CRDS	0.56−0.58		ppmv levels		pure gas
	86	pulsed CRDS	0.613	2×10^{-8}	50	minutes	NO_2/Ar mix
	32	broad-band CRDS	0.415−0.432		ppmv levels		
	87	pulsed CRDS	0.438−0.450		~3,000		engine exhaust
	88	CW CRDS	0.410	7×10^{-9}	0.4	15 s	NO_2/Ar mix
NO_3	93	CW CRDS	0.662	1×10^{-9}	0.002	30 s	lab source
	29	broad-band CRDS	0.65−0.67		0.0016	12 min	lab source
	97	pulsed CRDS	0.662	1.3×10^{-10}	0.0003	5 s	ambient air - field deployed
N_2O_5	95	CW CRDS	0.662	1×10^{-9}	0.0012	25	ambient air - field
	97	pulsed CRDS	0.662	1.3×10^{-10}	0.0003	5s	deployed
HONO	102	pulsed CRDS	0.354	2×10^{-8}	1.7		lab source
OH	14	pulsed CRDS	0.309		ppmv levels		heated air
	109	CEA/ICOS	1.51		ppmv levels		heated air
Hg	14	pulsed CRDS	0.254		0.001		lab air
	112	pulsed CRDS	0.254		0.001		lab source
	111	pulsed CRDS	0.254		0.0002	15 s	lab air
$^{13}CH_4$	114, 115	locked CW CRDS	3.3	2×10^{-9}	±11‰	minutes	lab air
$^{13}CO_2$	116	CW CRDS	1.6	3×10^{-11}	0.2 ‰	1 s	breath
$H_2{}^{18}O$	117	pulsed CRDS	0.95		7 ‰	900 s	standard
aerosol	119	pulsed CRDS	0.532	1×10^{-10}			ambient air
			0.355	6.6×10^{-7}			
	120	pulsed CRDS	0.532				flame
	121	pulsed CRDS	1.064	1×10^{-8}		5 s	ambient air
			0.532				
	123, 124	pulsed CRDS	0.510	3×10^{-9}		0.15 s	ambient air
			0.578				
	125	pulsed CRDS	0.620	8×10^{-8}		13 s	ambient air salt aerosol
	126	CW CRDS	0.69	1.5×10^{-8}		10 s	ambient air polystryrene spheres
			1.55				
	127	pulsed CRDS	0.532	1×10^{-9}		5 s	ambient air polystryene spheres

[a] Quoted sensitivity (α_{min}) scaled to 1σ noise level. [b] Minimum quoted detectable mixing ratio for 1σ noise limit. [c] Integration times not given by every author and are estimated in some cases. Integration times are taken as quoted, where available. In some cases, this is the time required for a acquisition of a single data point while in others for acquisition of a scan over an entire spectral line.

aerosol, a promising new field. Each section begins with a description of the atmospheric relevance and abundance of a particular class of compounds and gives sample, though not comprehensive, references to existing detection schemes. Table 1 summarizes the sensitivities, detection limits (in mixing ratio units), integration times, and sampling demonstrations of the various prototype instruments.

5.1. Methane, Hydrocarbons, and Formaldehyde

5.1.1. Methane

Methane is the most abundant hydrocarbon in the Earth's atmosphere, with a globally averaged surface mixing ratio of approximately 1.7 ppmv. It is also a potent greenhouse gas, and high-precision monitoring of methane over the long term at a variety of sites around the globe is of central importance in understanding climate change. Its routine measurement is via gas chromatography (GC),[50] although tunable diode laser (TDL) spectroscopy may be used, for example, in airborne measurements.[51,52] Because methane is a stable molecule without strong bands in the ultraviolet or visible, detection via CRDS or CEA/ICOS must take advantage of its rovibrational spectrum in the mid and near-IR. As noted above, Scherer et al.[47] demonstrated CRDS in the infrared region of the spectrum for the first time by recording a portion of the ν_3 (asymmetric C−H stretch band) of methane (lab sample) using a 10 Hz pulsed OPO that generated 3.5 ns pulses with a transform-limited line width.

More recently, several authors have demonstrated CH_4 detection, both in prepared gas mixtures and in sampling from ambient, laboratory air, using CW lasers. Fawcett et al.[53] scanned several different rovibrational lines near 1.65 μm ($2\nu_3$) using both an extended cavity diode laser (ECDL) and a distributed feedback (DFB) laser to pump a 45 cm cavity with a τ_0 value of ~9 μs. They used the standard cavity end mirror sweep method with a repetition rate of 10 Hz. The response of the instrument was linear over a range of $0.3-7 \times 10^{13}$ molecule cm^{-3} in low-pressure samples of premixed CH_4 in Ar. They also demonstrated detection of CH_4 in laboratory air at ambient pressure, where pressure-broadening effects limited the detection limit to 56 ppbv (parts per billion by volume), or $\alpha_{min} = 1.5 \times 10^{-8}$ cm^{-1} (1σ). Barry et al.[54] recorded the CH_4 absorption spectrum near 1.73 μm using the ICOS method. Their cavity consisted of mirrors somewhat lower in reflectivity, $R = 99.8\%$, separated by approximately 1 m. They observed an absorption signal from methane seeded in Ar at a total pressure near 20 Torr. The tuning range of the laser source did not permit observation of the strongest part of the $2\upsilon_3$ band, as in the Fawcett et al.[53] measurement, and even their predicted sensitivity in the stronger bands amounted to only 600 ppbv based on $\alpha_{min} \approx 1.8 \times 10^{-7}$ cm^{-1} from their (1σ) baseline noise estimate. Finally, Baer et al.[43] employed the off-axis cavity-integrated technique (OAICOS) to measure absorption spectra of a variety of trace gases in the near-IR, including CH_4 near 1.65 μm. They used a diode laser to pump an ~80 cm cavity with mirrors of $T = 400$ ppm at 1.65 μm, and they calibrated their cavity loss using a ring-down measurement ($\tau_0 \approx 7$ μs). They reported a rather impressive typical sensitivity of $\alpha_{min} = 3 \times 10^{-11}$ cm^{-1} Hz$^{-1/2}$ in their study that tested detection of several different trace gases with the same instrument. Their measurement of CH_4 in ambient air sampled from their laboratory appears in Figure 3. The 1 ppbv detection limit (S:N = 3) compares favorably with current diode laser conventional spectroscopic detection that gives roughly a 2 ppbv sensitivity under similar conditions.[52] They were able to determine the CH_4 mixing ratio in the lab air sample as 1.8 ppmv, consistent with globally averaged CH_4 levels.

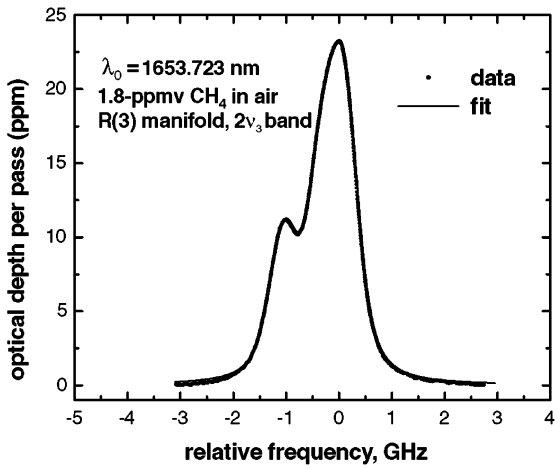

Figure 3. OAICOS absorption measurement of CH_4 in ambient air sampled in Mountain View, CA. The spectrum was obtained from a 600 sweep average by tuning a diode laser over three overlapping transitions (R(3) manifold, $2\nu_3$ band) near 1653.7 nm at a 600 Hz repetition rate for a 1 s integration time. The CH_4 detection limit was approximately 1 ppbv (S/N = 3). (Reprinted with permission from ref 43. Copyright 2002 Springer Verlag.)

5.1.2. Hydrocarbons

Larger hydrocarbons play an important role in atmospheric chemistry and radiative forcing, although they are present in significantly smaller abundances than CH_4 because of their short atmospheric lifetime with respect to reaction with OH and other oxidants. There are any number of current detection schemes for these compounds,[55] but common techniques include gas chromatography and, recently, proton-transfer-reaction mass spectrometry (PTR-MS).[56] At least for smaller hydrocarbons, spectroscopic approaches offer specificity for particular compounds. There are several proof of concept examples of HFCAS detection of small hydrocarbons (i.e., chain length of two) in ambient samples, including ethane, ethylene, and acetylene, along with a smaller number of attempts at detection of larger compounds.

Dahnke et al.[57] showed the detection of ethane from samples of human breath using their mid-IR CRDS spectrometer. The detector was based on a CO overtone laser (not portable) with tunable sidebands whose frequency (near 3.3 μm) was locked to a 55 cm cavity with $T = 100$ ppm mirrors. Their detection sensitivity was approximately 10^{-9} cm^{-1} for a 2 s integration, although scanning over a single line in the ethane spectrum required approximately 20 such measurements. Their estimated detection sensitivity at a single frequency point was 0.1 ppbv (0.5 ppbv including long-term instrument drifts). They noted that there would be significant interference problems from other absorbers, particularly isoprene, so their analysis required removal of less volatile compounds by cryogenic trapping prior to sampling and working

at a sample pressure of 100 mbar to reduce spectral overlap of pressure broadened lines. Interestingly, they were able to show the increase in ethane concentrations in exhaled breath from a human subject who had recently smoked a cigarette. Although the goal of this study was to demonstrate a medical rather than an atmospheric application, analysis of human breath samples provides an environment similar to, and at least as challenging as, ambient air.

Several authors have demonstrated detection of ethylene (C_2H_4) for mid-IR HFCAS proof of concept measurements in the spectral region near 10 μm. Although these studies were done with large, nonportable laser systems, the intent was for development of atmospheric trace gas detection in this region. Mürtz et al.[16] used a 3.5 kHz bandwidth CO_2 laser source locked to a cavity with mirrors of 99.5% reflectivity to achieve τ_0 values of approximately 1.3 μs. The 1σ variability in this time constant (for 5s averages) gave $\Delta\tau_{min}/\tau_0$ of 10^{-3} and $\alpha_{min} \approx 3 \times 10^{-8}$ cm^{-1} and a detection limit for ethylene of 1 ppbv via absorption near 10.6 μm. In this laboratory study, they used mixtures of ethylene in pure nitrogen and noted several improvements that would increase the sensitivity, including mirror reflectivity and signal acquisition. Bucher et al.[58] used a similar detection scheme for ethylene in the same spectral region to demonstrate saturation effects, which can be significant for locked, CW pumped cavities that have large running power. Peeters et al.[59] also used the ethylene absorption spectrum at 10.5 μm for demonstration of cavity-enhanced absorption (CEA) in this spectral region. Their cavity was 19 cm in length with mirrors of 99.92% reflectivity, and the detection sensitivity was $\alpha_{min} = 1.5 \times 10^{-6}$ cm^{-1} or 5 ppbv for ethylene probed on a single line output of the CO_2 laser. The analysis was done on mixtures of ethylene in nitrogen at atmospheric pressure rather than in ambient air. Parkes et al.[60] recently showed detection of ethylene using a near-IR CW diode laser source near 1.6 μm to pump a 45 cm cavity with τ_0 in the range 7−11 μs and $\alpha_{min} = 1.3 \times 10^{-8}$ cm^{-1}. The data acquisition routine was a standard piezoelectric cavity sweep (10 Hz repetition rate), although in some cases they swept the laser frequency at fixed cavity length. They obtained a detection limit equivalent to 78 ppbv in a low-pressure sample of dilute ethylene/Ar in a vacuum chamber measurement with a 30−90 s integration time and a zero obtained by removing the sample from the chamber. They noted that the quoted sensitivity may be degraded at atmospheric pressure and that the sensitivity is insufficient for detection in ambient air. They discussed several potential improvements to the system to make it viable for detection of larger volatile organic compounds (VOC), including the use of mid-IR wavelengths, longer cavities, higher reflectivity mirrors, faster sample acquisition, higher oscilloscope bit resolution (8 bits in this study), and sample preconcentration schemes.

Acetylene (C_2H_2) has been another common demonstration gas for near- and mid-IR HFCAS experiments. In the same study noted above for methane detection, Scherer et al.[47] used near-infrared detection of acetylene near 1.6 μm ($\nu_1+\nu_3$ band, or first C−H stretch overtone). Using the same OPO light source described above and a cavity with $T = 100$ ppm mirrors they achieved a detection sensitivity of 5×10^{-8} cm^{-1}. Awtry et al.[61] reported the development of a detector to monitor air quality aboard spacecraft. A CRDS scheme based on near-IR diode lasers fit their criterion for versatility of detectable species and sensitivity. They used acetylene as one of several test compounds. Their laser source was a 5 mW, 5 MHz extended cavity diode laser (ECDL) operating near 1.5 μm, and their cavity was 26 cm in length with low transmission mirrors, $T \approx 70$ ppm ($\tau_0 = 12-15$ μs). Using a standard cavity sweep method at 75 Hz to achieve periodic resonances with the laser source, they achieved $\alpha_{min} \approx 10^{-9}$ cm^{-1}, sufficient for a detection limit of 4 ppbv for acetylene (and 8 ppbv for HCN). They demonstrated the detection by sampling these gases from a methane/air pyridine flame, observing agreement with previous mass spectrometry calibrations of C_2H_2 concentrations in similar flames to within 1%. The instrument described by Parkes et al.[60] for near-IR ethylene measurements (see above) was also applied to measurement of acetylene near 1.5 μm with a low-pressure detection limit of 0.88 ppbv and an ambient pressure estimate of 6 ppbv. The former level is sufficient for ambient detection of this compound. Finally, the OAICOS study of Baer et al.,[43] described above for CH_4, achieved a detection sensitivity for C_2H_2 of 0.3 ppbv in a 1 s average (3σ) at 1.53 μm. The sample was a mixture of acetylene in pure N_2 at 50 Torr, and the authors noted the potential for interferences from other absorbers at this wavelength in a real air sample, from, for example, a monitor in an industrial setting.

There are a few examples of the application of HFCAS to the detection of larger organic molecules. The spectroscopy of such compounds does not generally allow for single rovibrational line detection, as in the cases cited above for one- and two-carbon organics. Spectroscopic specificity may become an issue as a result, particularly with respect to resolving a particular compound in the presence of competing absorptions. Parkes et al.[60] present a discussion of these difficulties, which are common to any spectroscopic approach to the detection of larger molecules. These authors demonstrated CRDS detection of 1,3-butadiene, 1-butene, and 2-methylpropene in Ar mixtures with sensitivities of 900, 1600, and 4200 ppbv, respectively. One example that is particularly relevant in light of recent events is the development of a CRDS-based detector for vapor from explosives. Todd et al.[62] developed a mid-IR pulsed OPO laser source specifically for this purpose. The OPO, based on pumping a zinc−germanium−phosphide (ZGP) crystal with a Q-switched erbium, chromium-doped yttrium−scandium−gallium−garnet (Er, Cr:YSGG) laser at 2.8 μm, produced tunable pulses of 100 ns duration over the range 6−8 μm with a typical line width of 2 cm^{-1}. Their cavity consisted of low-transmission mirrors, $T = 40$ ppm, separated by 50 cm, though only the central 10 cm of the cavity was used for the sample gas. This spectrometer was well-

suited to the mid-IR vapor-phase absorptions of compounds such as TNT (and several others), which exhibit broad bands with structure that varies slowly with wavelength between 7 and 8 μm. The sensitivity was 9×10^{-9} cm^{-1} Hz$^{-1/2}$ at a single wavelength point. A comparison of instrument detection sensitivity to that required based on the room-temperature vapor pressures of TNT was favorable, although chemical preconcentration would be necessary for detection of other explosive vapors. Finally, Vasudev et al.[15] used pulsed CRDS in the ultraviolet as a means of detecting chlorinated aromatic compounds, whose sensitive environmental monitoring would be of some significance due to the prevalence of pollutants such as dioxins. They pumped a 24 cm cavity comprised of fairly low reflectivity mirrors with the 266-nm fourth harmonic of a Nd:YAG to probe chlorobenzene and 1,3-dichlorobenzene on electronic transitions. This approach achieved only part per million sensitivity levels in premixed samples without much specificity to these particular compounds at this single wavelength, highlighting the difficulty of CRDS detection in the UV.

5.1.3. Formaldehyde

The simplest example of an oxygenated organic is formaldehyde, and its chemistry is extremely important in the atmosphere, where it ranges from 0.05 to 60 ppbv due to both hydrocarbon oxidation and direct emissions.[63] Currently available detection schemes for this compound include DOAS[64,65] for long open-path detection and tunable diode laser spectroscopy, with detection limits of a few tens of parts per trillion, for in situ measurements (see, for example, Fried et al.[66] and Kormann et al.[67]). Formaldehyde has a strong, characteristic, structured UV absorption spectrum in addition to well-resolved rovibrational lines in the mid- and near-IR. Three examples of prototype instruments for atmospheric sensing of CH_2O using direct absorption in high-finesse cavities have taken advantage of each of these spectral regions. However, none of the HFCAS-based prototypes have yet achieved detection sensitivities comparable to that achieved by TDLS (see above), and field tests have yet to be reported. Kleine et al.[44] measured the UV absorption spectrum of a mixture of 24 ppmv of CH_2O in air between 312 and 327 nm and determined a detection limit of roughly 300 ppbv. They used a frequency-doubled, tunable dye laser to pump a cavity comprised of $R = 99.7\%$ mirrors separated by 50 cm and obtained a sensitivity of $\alpha_{min} = 4 \times 10^{-7}$ cm^{-1}. They pointed out that this sensitivity was not useful for ambient detection and was limited by the availability of sufficiently reflective UV mirrors and Rayleigh scattering losses. In a study that was experimentally quite similar to their methane measurements described above,[54] Barry et al.[68] measured the absorption cross sections of CH_2O in the first asymmetric C−H stretch overtone ($2\nu_5$) near 1.76 μm using the CEA approach. They found the overtone intensity to be slightly more than 2 orders of magnitude smaller than that of the fundamental. They went on to calculate the feasibility for CH_2O detection in ambient air using a CEA spectrometer with an assumed sensitivity of 10^{-8} cm^{-1} to arrive at a presumed detection limit of 350 ppbv, well short of that needed for ambient detection. Finally, Dahnke et al.[69] demonstrated CH_2O detection in a cavity with a τ_0 value of $\sim$4 μs ($T \approx 500$ ppm mirrors). Their light source was a tunable CO overtone laser at 3.5 μm (ν_5 fundamental) that was actively locked to the cavity. Acquisition of ring-down transients at 500 Hz gave $\alpha_{min} = 7 \times 10^{-9}$ cm^{-1} Hz$^{-1/2}$ for a CH_2O detection limit of 2 ppbv. They demonstrated the detection in ambient air samples (total pressure of 30 mbar) artificially doped with CH_2O at levels from 8 to 280 ppbv. The authors pointed out that the laser source used in this study was large, confined to the laboratory, and did not have a tuning range that encompassed the strongest CH_2O lines in this region. They predicted a CH_2O detection limit of 150 pptv for a 1s average in a portable instrument with a more versatile laser source (and slightly better mirror reflectivity), although they did not consider zero measurements or sampling issues explicitly.

5.2. Carbon Monoxide and Carbon Dioxide

Carbon dioxide is the most important greenhouse gas, and its mixing ratio has increased steadily throughout the industrial period to reach a 1999 level of 367 ppm.[70] Carbon monoxide, on the other hand, occurs at highly variable levels, in the range 0.1−10 ppmv depending on the proximity to major sources (i.e., urban areas).[63] Common detection methods for CO and CO_2 detection include gas filter correlation nondispersive infrared (NDIR) measurements (i.e., measurement of heat deposited by a broad-band IR source in a sample cell compared to a reference cell containing a pure gas), which offer the advantage of simplicity,[71,72] and TDL absorption spectroscopy, which offers greater specificity.[73] Such techniques offer sensitivities in the range 0.1−1 ppbv with measurement precision of a few percent. Because of their relatively large abundances, both CO and CO_2 should be readily detectable in ambient air using a high-sensitivity schemes such as CRDS and CEA ICOS. The main advantage in doing is for applications requiring high precision, e.g., for assessing trends, making flux measurements, or examining isotopic enrichment (see below). Since they are noncondensable, stable gases, sampling issues are less significant than for gases such as formaldehyde.

Several recent examples of CRDS and CEA/ICOS instruments designed specifically for trace gas detection have exploited the CO and CO_2 absorption spectra in the near-IR around 1.5 μm. He and Orr[74] described a CRDS instrument using their rapidly swept cavity scheme combined with optical heterodyne detection that was designed for ambient trace gas monitoring in the near-IR Their resulting sensitivity was $\alpha_{min} = 2.5 \times 10^{-9}$ cm^{-1} Hz$^{-1/2}$, and they demonstrated the detection by scanning over several absorption lines in 50 mbar of pure CO_2 gas (scan wavelength near 1.53 μm). The spacecraft air quality monitor of Awtry et al.[61] achieved limits of 2 and 2.5 ppmv (S:N = 3) for CO and CO_2, respectively, in test scans near 1.57 μm. They sampled CO_2 from the air in their laboratory at total pressures from 5 to 80 Torr and obtained an average mixing ratio of 453 ±

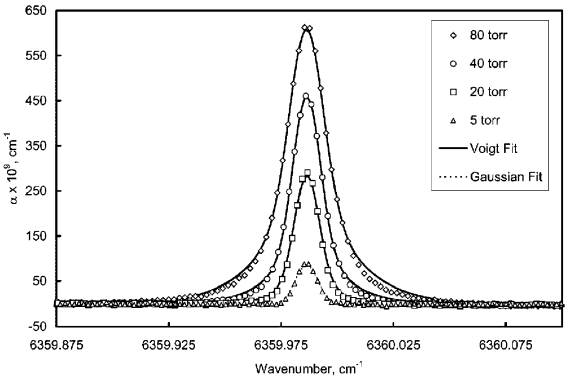

Figure 4. A series of CO_2 absorption measurements at different pressures obtained using CW CRDS. All peaks were fit to a Voigt line shape with the exception of the 5 Torr peak, which was fit to a Gaussian. The fits give an ambient concentration of 453 ± 7 ppm. (Reprinted with permission from ref 61. Copyright 2002 Springer Verlag.)

7 ppmv. Figure 4 shows a set of scans of a single CO_2 line at a series of pressures from this study. The Baer et al.[43] OAICOS measurement presented scans over near-IR rovibrational lines of both CO_2 and CO. The detection sensitivity for the latter, sampled again from ambient, laboratory air, was 36 ppbv for S:N = 3 in a 1s average using a single line in the second overtone band at 1.56 μm.

5.3. Ammonia

Ammonia is important to the formation and growth of atmospheric aerosol because it reacts readily with gas-phase acids (e.g., HNO_3, H_2SO_4) and acidic particles to produce condensable ammonium salts. It ranges from <0.1 to as much as 60 ppbv as a result largely of emissions from agricultural sources.[63] Although there are any number of detection schemes for atmospheric ammonia, its gas-phase measurement is difficult and ambient levels remain poorly characterized.[75] Denuder systems (i.e., a device that absorbs NH_3 out of the gas phase for wet chemical analysis) are a common standard method, although other methods, including direct absorption, chemiluminescent schemes, mass spectrometry, photothermal interferometry, etc., have been developed, tested, and intercompared.[75−79] These systems have typical sensitivities in the range 25−200 pptv. One of the principle difficulties is the affinity of NH_3 for the surfaces of any in situ, real-time detector. Since CRDS is also an in-situ method, it will suffer from the same difficulty unless, for example, its detection path can be left open to the atmosphere (see below).

In a series of papers beginning in 1995, Meijer and co-workers examined several different detection schemes for ammonia using both CRDS and CEA. Jongma et al.,[14] who also examined both OH and Hg (see below), demonstrated the first detection of NH_3 via CRDS with a pulsed laser in the ultraviolet. They frequency tripled the output of a tunable pulsed dye laser to obtain UV light near 204 nm for probing the strong (A ← X) electronic transition in NH_3. Their cavity was 45 cm in length and formed by mirrors of 98.5% reflectivity. They observed absorption in a calibrated flow of NH_3 in air to deduce a detection limit of roughly 10 ppbv. The same research group revisited NH_3 detection in their initial description of the CEA concept.[8] Using a 90 cm cavity with R = 99.92% mirrors pumped by a diode laser at 1.52 μm, they obtained the spectrum of several weak NH_3 lines in a low-pressure mixture of water vapor with trace quantities of ammonia. On the basis of the noise level, they predicted a sensitivity of roughly 10^{-6} mbar (or approximately 1 ppbv for NH_3 if the result can be scaled to atmospheric pressure) on stronger lines in the same region. They also showed the application of CEA spectroscopy to the measurement of NH_3 in a pulsed supersonic expansion.[13] In a more detailed feasibility study of CEA detection of NH_3, Peeters et al.[80] again recorded a portion of the 1.5 μm NH_3 absorption spectrum using an open path at atmospheric pressure inside of a climate chamber. The open-path detection served to eliminate inlet effects in the sampling of ammonia from the atmosphere; nevertheless, in this lab study, there were still artifacts due to adhesion of NH_3 to the climate chamber surfaces. They calibrated the losses in their 67 cm cavity based on known, water vapor standards and reported a sensitivity of 2×10^{-8} cm^{-1} Hz$^{-1/2}$ (1σ), corresponding to an NH_3 detection limit of only 100 ppbv. Better predicted limits could be attained on stronger (~5×) lines near 2 μm, and even better detection limits in the mid-IR, presuming availability of light sources.

Paldus et al.[48] were in fact able to realize mid-IR detection of NH_3 to achieve substantially better sensitivity. They used a cryogenically cooled (35−60 K) quantum cascade (QC) laser at 8.5 μm to pump a three-mirror cavity with a round trip length of 45 cm and mirrors of 99.97% reflectivity (τ_0 values slightly less than 1 μs). By sweeping one of the cavity mirrors sinusoidally through one free spectral range at a rate of 300 Hz, they were able to record ring-down transients at 600 Hz and achieve a noise limit of 4×10^{-9} cm^{-1} Hz$^{-1/2}$. They introduced samples of NH_3 in N_2 into their cavity, scanned a single rotational line, and arrived at a detection sensitivity of 0.25 ppbv. Ammonia was also one of the test gases for the spacecraft air quality monitor prototype of Awtry et al.[61] described above. They reported a detection limit of 19 ppbv in the near-infrared bands near 1.5 μm (sensitivity was $\alpha_{min} \approx 10^{-9}$ cm^{-1}). Finally, the recent OAICOS study of Baer et al.[43] reported near-IR (1.53 μm) sensitivity for NH_3 of 2 ppbv (at S:N = 3) in a 1s average. Their sample scan over a single NH_3 absorption line came from a mixture of room air doped with 5 ppmv of NH_3 from a cylinder at a total pressure of 100 Torr. None of these studies examined sampling or inlet effects for NH_3 in any great detail, and only the mid-IR scheme has achieved a sensitivity competitive with existing instrumentation (see above).

5.4. Nitrogen Oxides

5.4.1. NO and NO_2

Nitrogen oxides constitute an important class of atmospheric trace compounds. The pair of molecules, NO and NO_2, commonly referred to as NO_x, regulates the abundance of ozone in all levels of the atmo-

sphere. Sensitive instruments capable of measuring their mixing ratios, which range from tens of pptv in clean air to hundreds of ppbv under severely polluted conditions, are important. Both compounds are readily detected via chemiluminescence methods in which the reaction of NO with O_3 yields electronically excited NO_2*, whose fluorescence provides the detection signal.[81] (Detection of NO_2 via this method proceeds by prior conversion to NO by, for example, photolysis.) These methods have achieved sensitivities on the order of 10 pptv.[82] Other similarly sensitive methods include laser-induced fluorescence detection for NO_2.[83]

There are two examples of NO detection in the mid-IR by the same research group, one using CRDS and the other using CEA. Both examples were based on a liquid nitrogen cooled quantum cascade laser used to probe the NO fundamental vibrational transition at 5.2 μm. The goal of each study was to develop a device for medical diagnostics (i.e., determining NO concentrations in breath samples) rather than for atmospheric monitoring. Menzel et al.[84] made a side by side comparison of the CEA technique with a multipass (Herriot) cell. For the CEA arrangement, they used a 36 cm cavity with mirrors that had a specified transmission of 50 ppm at 5.2 μm but an actual, calibrated transmission (measured from the intensity of known CO_2 lines in the same region) of 600 ppm. The resulting effective path length was 670 m, and they found a detection limit for NO of 16 ppbv, limited mainly by the residual intensity noise after averaging of many successive scans. They demonstrated the detection in a human breath sample at a total pressure of 30 Torr, where the actual NO mixing ratio was 70 ppbv. The CEA measurement compared poorly with the multipass cell, which had a path length of only 100 m but 2 orders of magnitude smaller intensity noise for an NO detection limit of only 3 ppbv at the same wavelength. Kosterev et al.[49] used a similar, 37 cm length cavity for the ring-down measurement of NO at 5.2 μm, with τ_0 values of 3.5 μs (mirror transmission $T = 350$ ppm). They swept the cavity through four free spectral ranges to acquire ring-down transients at 1.6 kHz. They obtained a sensitivity of $\alpha_{min} = 5 \times 10^{-8}$ cm^{-1} and a minimum detectable NO mixing ratio of 0.7 ppbv in an 8 s average from a measurement of an NO sample from a cylinder diluted in dry N_2. The detection from a breath sample was unsuccessful because of interferences from CO_2 and water vapor lines, even at a reduced pressure of 60 Torr. The authors speculated that a different, nearby NO line (inaccessible with their laser source) would make the breath measurement feasible.

Nitrogen dioxide was the first example (other than water vapor) of trace gas detection in the ambient atmosphere via CRDS. O'Keefe et al.[12,85] recorded a CRDS spectrum of NO_2 in ambient, laboratory air between 425 and 460 nm using a tunable, pulsed dye laser. Their cavity was 100 cm in length with $T = 20$ ppm mirrors. They observed the characteristic absorption spectrum of NO_2 and determined a mixing ratio of 16 ppbv (scan acquisition time of minutes). Vasudev et al.,[15] in the same study described above for chlorinated organics, also suggested the use of a visible wavelength, pulsed tunable dye laser CRDS system as an environmental detector for NO_2. They demonstrated sensitivity of only a few ppmv, insufficient for this purpose, but they suggested improvements to achieve ppbv level sensitivity. In a similar study, Lauterbach et al.[86] were able to achieve ppb level sensitivity to NO_2 using pulsed CRDS detection from 595 to 630 nm. They used a 45 cm cavity and obtained a baseline noise level of 2×10^{-8} cm^{-1} in 1 atm of air, enough for a sensitivity of roughly 50 ppbv at the absorption maximum at 612.9 nm. They noted that the NO_2 absorption spectrum near 430 nm is approximately 4$\times$ more intense. However, zero levels were recorded by removing NO_2 from the absorption cell rather than by scanning over a portion of the spectrum. Czyzewski et al.[32] applied a pulsed, broadband CRDS technique to the detection of NO_2 at mixing ratios of approximately 10 ppmv. Using a pulsed CRDS apparatus and UV and visible wavelengths, Evertsen et al.[87] measured both NO and NO_2 concentrations in diesel engine exhaust. They used the UV bands of NO near 226 nm and the visible absorption spectrum of NO_2 between 438 and 450 nm. The light source was either the fundamental (visible) or frequency-doubled (UV) output of a tunable dye laser. The optical cavity was 45 cm in length, but owing to the very large absorption from the high NO_x concentrations from the engine, it was necessary to inject sample gas only into the central 1.2 cm of this path. Soot filters reduced the impact of Mie scattering. The NO and NO_2 levels were 222 and 29 ppmv, respectively, and the measurement precision, determined from a scan over several nm in each absorption spectrum (requiring $\sim$7 min acquisition time), was roughly 10$-$13%. This approach has sufficient sensitivity for the very large NO_x concentrations in a direct exhaust stream but would be inappropriate for general environmental monitoring.

Recently, Mazurenka et al.[88] demonstrated NO_2 detection at 410 nm using a blue CW diode laser and a standard piezoelectric sweep (sweep rate of 500 Hz) with an AOM switch. They measured absorption spectra of dilute NO_2/Ar mixtures at total pressures between 1 and 10 Torr both to determine absorption cross sections and to examine the feasibility of ambient NO_2 detection. The time constant in their 35 cm cavity was $\tau_0 = 26$ μs at low pressure for a sensitivity of $\alpha_{min} = 7 \times 10^{-9}$ cm^{-1} (15 s average). This limit will be degraded somewhat at higher pressures by Rayleigh losses, and these authors also did not detail an accurate zero determination scheme for ambient measurements. Kasyutich et al.[89] also observed NO_2 absorption using a blue CW diode laser at 404 nm. They used the off-axis ICOS approach in an apparatus intended primarily for chemical kinetics studies rather than atmospheric monitoring. Their sensitivity was equivalent to a 700 pptv detection limit.

Although the detection limits in all of the foregoing NO_2 HFCAS detectors are rather large, straightforward improvements outlined by several of these authors combined with a well-crafted zero determination scheme should achieve more useful detection

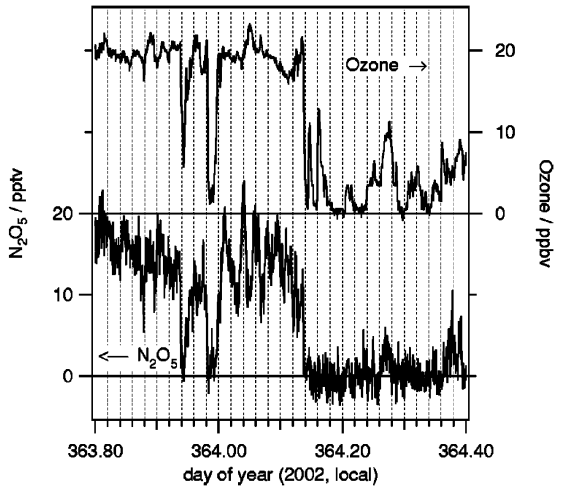

Figure 5. Time series of ambient O_3 (measured with a commercial instrument) and N_2O_5 (measured by CW CRDS at 662 nm) mixing ratios obtained near midnight, December 29−30, 2002, in Fairbanks, AK. The correlation between O_3 and N_2O_5 mixing ratios suggests loading of NO in the O_3 poor air that titrates the O_3 and also suppresses formation of N_2O_5. (Reprinted with permission from ref 95. Copyright 2003 American Institute of Physics.)

sensitivities on the order of tens of pptv with a rapid time response.

5.4.2. NO_3 and N_2O_5

The higher oxides of nitrogen, NO_3 and N_2O_5, are unimportant in the atmosphere during the day due to the rapid solar photolysis of NO_3 and its reaction with NO but build to appreciable concentrations at night. The abundances of NO_3 and N_2O_5 are several pptv to several ppbv, respectively, and are of interest since NO_3 is an important oxidant and since heterogeneous hydrolysis of N_2O_5 is an important pathway for the conversion of NO_x to nitric acid. NO_3 has characteristic strong visible absorption bands, with a maximum near 662 nm, and has been most commonly detected in the atmosphere using long-path DOAS methods.[90,91] No detection scheme (other than IR remote sensing in the stratosphere[92]) has been available for N_2O_5.

Several studies, including our own, have been aimed at the detection of NO_3 via HFCAS. Each study has employed a very different experimental approach. King et al.[93] used an ECDL at 662 nm to pump a four-mirror bow-tie cavity with mirrors of 40 ppm transmission. They achieved laser to cavity resonance by modulation of the laser frequency around each cavity mode. They recorded ring-down transients at a rate of 5 Hz and obtained a sensitivity of $\alpha_{min} = 10^{-9}$ cm^{-1} in a 30 s average, enough for a 2 pptv detection sensitivity for NO_3, which has a strong absorption cross section (2.2×10^{-17} cm^2 molecule^{-1} at 662 nm[94]). The demonstrated detection by doping a flow of ambient air in their laboratory with N_2O_5, which thermally dissociates to give a variable quantity of NO_3. In a more recent demonstration of a field-ready prototype, Simpson[95] has shown ambient detection of N_2O_5 during winter in Fairbanks, AK, as shown in Figure 5. The instrument had operating characteristics and detection sensitivity similar to that listed above but was modular in design, with the cavity and sampling flow system mounted on a rail system that was fiber coupled to and physically separated from the laser source, detectors, and control electronics. They utilized a sampling system (halocarbon wax coated glass), zero detection scheme (NO titration), and heated inlet for thermal conversion of N_2O_5 to NO_3 that was similar to our NO_3 and N_2O_5 instrument (see below). They observed approximately 20 pptv ambient mixing ratios of N_2O_5 in Fairbanks.

In a rather different approach, Ball et al.[29] used the broad-band CRDS method, reviewed in this issue, for NO_3 detection. Their prototype achieved an estimated NO_3 detection limit of 1.6 pptv in a 12 min average based on laboratory studies.

In a series of recent papers,[96−98] our research group demonstrated the detection of NO_3 and N_2O_5 via pulsed CRDS. This instrument has two optical cavities of 95 cm with mirrors of $T \approx 10$ ppm (τ_0 value of $\sim$180 μs at atmospheric pressure, including Rayleigh scattering losses), and the light source is a small footprint Nd:YAG laser-pumped dye laser that supplies 3 mJ pulses at a repetition rate of 20 Hz. Performance testing of this instrument was carried out both in the laboratory and in the field, where fast response, in-situ detection of naturally occurring NO_3 was shown for the first time. Because NO_3 and N_2O_5 are in thermal equilibrium, heating the sampled air flow in the inlet converts N_2O_5 into NO_3; the increase in the NO_3 signal in a heated inlet and ring-down system gives a direct N_2O_5 concentration measurement, the first observation of this compound in the troposphere. The instrument currently consists of two optical cavities mounted side by side and pumped simultaneously from the same laser source. One cavity has a flow system that samples at ambient temperature, while the other is heated to 70−80 °C to convert N_2O_5 into NO_3. The 2σ sensitivities in both cavities is $\alpha_{min} = 2.6 \times 10^{-10}$ cm^{-1} for a 5 s integration (6×10^{-10} cm^{-1} Hz$^{-1/2}$) or 0.5 pptv mixing ratio for both compounds considering inlet sampling losses. Mie scattering from atmospheric aerosol greatly reduces the detection sensitivity; the instrument consequently requires a thin Teflon membrane filter at the inlet to remove large aerosol. This membrane also consumes 15 ± 5% of the ambient NO_3, an acceptable, though undesirable, sampling loss. This measurement capability has allowed new insights into the nocturnal chemistry of nitrogen oxides in studies at both a ground site near our laboratories in Boulder, CO,[98] where N_2O_5 mixing ratios up to 3000 pptv were observed, and in the marine boundary layer on board a ship (the R. V. Ronald H. Brown) off the East Coast of the United States.[99]

Finally, Kasyutich et al.[100] observed NO_3 radicals via 622 nm absorption in a recently reported off-axis ICOS arrangement. As in their companion study of NO_2 noted above, the intent was for laboratory kinetics studies. Nevertheless, they obtained a detection limit equivalent to 200 pptv (1σ) with a short (22 cm) cavity base path and mirrors of only 99.9% reflectivity.

5.4.3. HONO

The chemistry of nitrous acid, HONO, is closely related to that of the nitrogen oxides. It forms from the reaction of NO with OH radical and from the heterogeneous hydrolysis of NO_2[101] and occurs at levels up to 10 ppbv in polluted environments. Like NO_3 and N_2O_5, its concentration is most significant at night because of its degradation by near UV photolysis in sunlit air. Its photolysis can serve as an important source of OH at sunrise. Current detection schemes for HONO include DOAS[64,65] and wet chemical analysis.[63] Because of its strong, structured near-UV absorption spectrum, it is a potential candidate for monitoring with a CRDS instrument. Wang and Zhang[102] proposed to do just this in a laboratory feasibility study using a pulsed UV laser source. They pumped a 108 cm cavity with mirrors of 800 ppm transmittance ($\tau_0 \approx 2\ \mu$s) with a frequency-doubled dye laser at 354 nm, the peak of the HONO spectrum. They tested this instrument with a high-purity HONO source in clean air in their laboratory over a range of 12−400 ppbv. The detection sensitivity of $\alpha_{min} = 6 \times 10^{-8}$ cm^{-1} in a 15 s integration (3σ) gave a minimum detectable HONO mixing ratio of 5 ppbv for monitoring at a single wavelength point. They noted that the presence of interfering absorbers in this region could be overcome by use of differential spectroscopic techniques using short scans or two wavelength points to discern HONO from other UV absorbers. Although 5 ppbv is not a particularly useful detection limit for HONO, the authors outlined sensitivity improvements that could achieve sub-ppbv levels.

5.5. Hydroxyl Radical

The hydroxyl radical presents perhaps one of the most difficult challenges in atmospheric trace gas detection. It is among the most important atmospheric compounds, but, because of its reactivity, hydroxyl is also present in exceedingly small concentrations—of order 10^6-10^7 molecules cm^{-3} during daylight hours (i.e., ≤ 0.4 pptv). Current detection schemes for atmospheric OH[103] include DOAS,[104] for long, open-path detection, and in situ instruments based on fluorescence[105,106] and mass spectrometric techniques.[107] Although OH possesses strong near-UV absorption bands and has been seen repeatedly via HFCAS in flames (see, for example, Spaanjaars et al.[108]), an instrument with sufficient sensitivity for atmospheric OH detection in the near UV ($\alpha_{min} \leq 2 \times 10^{-10}$ cm^{-1} for ambient pressure detection[104]) has yet to be demonstrated.

Jongma et al.[14] were able to observe OH in heated air in the same pulsed CRDS apparatus described above for their study of UV absorption by NH_3. Their ambient pressure, 45 cm cavity had a τ_0 value of ∼0.3 μs at 309 nm, and an oven occupied the central 30 cm of the path length. Upon heating of laboratory air (relative humidity near 50%) to temperatures in the range 720−1125 K to induce thermal dissociation of water vapor, they recorded spectra of OH radicals at mixing ratios of several hundred to several thousand ppbv. More recently, the same research group performed a similar experiment using a near-IR diode laser to measure a CEA spectrum of OH in heated laboratory air.[109] In this case their cavity was 65 cm in length, with an oven that could be heated to 1500 K in the central 25 cm of this length. They pumped this cavity with a diode laser at 1.51 μm, where the estimated mirror transmission was 1000 ppm. They observed infrared lines assignable to OH at oven temperatures between 900 and 1500 K, with a measured OH mixing ratio at the high end of this temperature range of 44 ppmv.

Barry et al.[110] reported development of UV CW laser source applicable to CRDS or CEA detection of OH at 308 nm. They also noted one of the major complications to this approach, the formation of OH from the reaction of water vapor with O (^{1}D) formed from photolysis of ambient O_3 by the laser light within the cavity. This has been a complicating factor for LIF measurements of OH at ambient pressures and would certainly complicate in situ measurements by direct absorption, especially in a multipass configuration through the same sample volume. Any 308 nm HFCAS detection scheme for OH would likely have to be carried out at pressures low enough to suppress this artifact. Successful demonstration of an OH HFCAS instrument with sufficient sensitivity for ambient levels would be an interesting and useful development.

5.6. Elemental Mercury

The toxicity of mercury is well-known. It occurs as an airborne pollutant at background mixing ratios of a few pptv, having a lifetime in the atmosphere of approximately 1 year with respect to deposition. It possesses a strong absorption line near 254 nm whose peak cross section, 3.3×10^{-14} cm^2 at atmospheric pressure,[14,111] is orders of magnitude larger than any of the molecular absorbers considered above. Despite the difficulty associated with UV CRDS ambient trace gas detection, Hg stands out as an ultraviolet absorber whose detection via this method is rather facile. Three different research groups have demonstrated useful detection limits and ambient sampling of Hg in pulsed CRDS approaches. As early as 1995, Jongma et al.[14] detected a mixing ratio of 7 pptv of Hg in air sampled from their laboratory using the same apparatus described above for pulsed, UV detection of NH_3 and OH. Using a 45 cm cavity with mirrors of $R = 99.6\%$, their τ_0 value was ∼0.33 μs, including Rayleigh (and presumably Mie) scattering losses and losses due to ambient O_3 absorption. They estimated their detection sensitivity at <1pptv. Tao et al.[112] also measured absorption due to gas-phase, elemental mercury in a pulsed CRDS spectrometer using a laboratory Hg source. Their instrument consisted of a 56 cm cavity with $R = 99.7\%$ mirrors pumped by the frequency-doubled output of a 20 Hz Nd:YAG laser pumped dye laser. With a τ_0 value of ∼0.7 μs, they obtained a 3σ detection limit for gas-phase Hg of 3 pptv. Spuler et al.[111] used a similar apparatus and laser source. With a τ_0 value of approximately 1.4 μs (including all losses in ambient air at 254 nm), they could achieve a 3σ detection sensitivity of 0.5 pptv for Hg. They observed a mixing

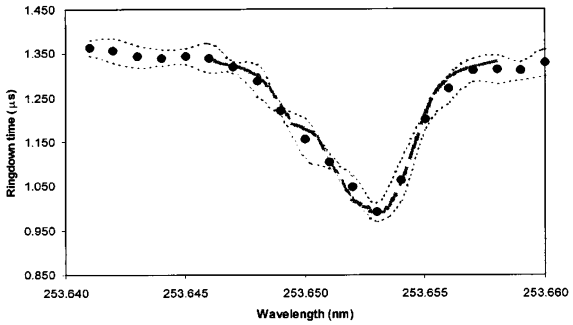

Figure 6. Ring-down time constant vs wavelength (points) for a scan of the Hg absorption line from 253.64 to 254.66 nm using pulsed CRDS. The solid line is the calculated, pressure-broadened Hg line, which consists of several overlapping transitions. The sample is ambient, laboratory air in the Denver, CO, area, and the Hg concentration is determined as 13 pptv. (Reprinted with permission from ref 111. Copyright 2000 Optical Society of America.)

ratio of 13 pptv Hg in laboratory air in the Denver, CO, area, as Figure 6 shows. These authors also considered the detection of other mercury compounds such as Hg_2Cl_2 and the effects of interferences due to background absorbers such as O_3 and SO_2, which were not significant. These three CRDS-based gas-phase Hg detectors are relatively similar and show considerable promise for the construction of a light-weight, rapid response, in-situ monitor for atmospheric Hg contamination.

5.7. Isotope Ratios

An obvious and extremely valuable application of a high-sensitivity, high-precision optical trace gas detector is in the measurement of isotopic ratios of small molecules. Isotopic enrichment studies require not only sensitivity sufficient to observe the smaller concentrations of more abundant compounds but also the measurement precision to accurately quantify relative abundances. Isotopic enrichment is defined as the difference in the ratio of two isotopomers in a sample and a standard divided by the ratio in the standard and is normally expressed in units of per mil (‰). Atmospheric isotopic enrichment studies are useful in distinguishing different sources for trace gases (e.g., anthropogenic vs biogenic) and in studying fractionation processes that occur within the atmosphere. The current state of the art method for such studies is isotopic ratio mass spectrometry (IRMS), which may also be combined with gas chromatography (see, for example, Miller et al.[113]). A high-sensitivity absorption scheme may offer several advantages to IRMS, including a more compact instrument design, smaller gas sampling requirements, and, importantly, the ability to easily distinguish isotopomers of the same mass (e.g., $^{13}CH_4$ from $^{12}CH_3D$) based on their unique rovibrational absorption spectra.

There are three separate reports of the measurement of $\delta^{13}C$ from methane in ambient air from the same research group.[44,114,115] Their apparatus was similar to the one described above for the measurement of ethane in breath samples using a mid-IR CRDS scheme.[57] They actively locked the frequency of a tunable sideband CO laser near 3.3 μm to a

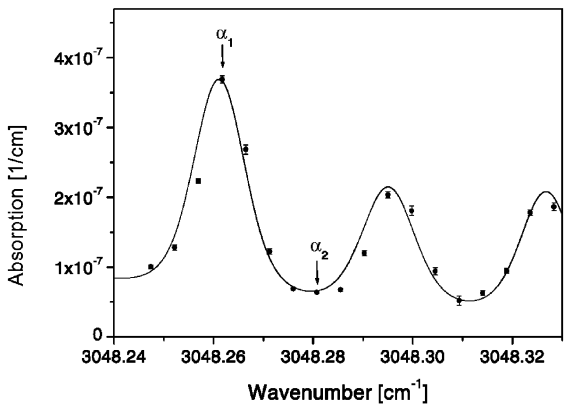

Figure 7. Scan of the $^{13}CH_4$ absorption spectrum in ambient, laboratory air (sampled at 50 mbar). The points are experimental data, and the solid line is a calculated spectrum from the HITRAN database at a $^{13}CH_4$ mixing ratio of 21 ppbv. (Reprinted with permission from ref 115. Copyright 2001 Springer Verlag.)

single mode in a 53 cm cavity with mirrors of 200 ppm transmission ($\tau_0 = 7.25$ μs). A 20 s integration time (average of 1000 ring-down events) yielded a 2σ sensitivity of 4×10^{-9} cm^{-1}. As Figure 7 illustrates, they were able to discern a mixing ratio of 21 ppbv of $^{13}CH_4$ in a 50 mbar sample of laboratory air (detection limit of 210 pptv). By scanning over two separate spectral regions, one containing a weak $^{12}CH_4$ line and one with a strong $^{13}CH_4$ transition, they extracted an isotopic enrichment of $\delta^{13}C = -45 \pm 11$‰. This value was in good agreement with the expected -47 ± 2‰ from an air sample in Germany. These authors reported that the precision of the measurement was a factor of 4 better than the best previous reported $\delta^{13}C$ measurement using a direct absorption technique. It was not as good as the best reported precision from IRMS studies nor was it sufficient to track changes in $\delta^{13}C$ of ± 2‰ in remote locations.

A recent example of $\delta^{13}C$ measurement in CO_2 using CRDS was the work of Crosson et al.[116] They used a near-IR diode laser at 1.6 μm to pump a three-mirror, 42 cm round trip path length cavity. They used a standard end mirror sweep scheme to bring cavity modes into resonance with a laser frequency but increased the signal acquisition rate using a tracking circuit that reversed the direction of the PZT immediately after each resonance. The resulting ring-down sampling rate was 1 kHz, and the detection sensitivity was 3×10^{-11} cm^{-1} Hz$^{-1/2}$. As in the study above, they scanned lines in the $^{13}CO_2$ and $^{12}CO_2$ spectrum that had comparable strengths but originated in different rotational states, making the measurement temperature dependent. Total sample pressures ranged from 5 to 70 Torr. Measurements of $\delta^{13}C$ in several samples compared favorably to measurements of the same samples using an IRMS instrument. They reported their precision to be approximately equal to that from a "typical" IRMS measurement, or ± 0.2‰, though not as good as state of the art IRMS measurements that can reach ± 0.01‰. They also compared human breath samples from subjects who were known to have tested either positive or negative for the presence of a bacteria that

causes stomach ulcers. The $\delta^{13}C$ measurements are a signature for this bacteria, and the CRDS measurements were easily sufficient to distinguish between positive and negative subjects.

Finally, Samura et al.[117] were able to measure the $\delta^{18}O$ values in water vapor samples using a conventional pulsed CRDS detection scheme (950 nm dye laser to probe the water vapor overtone spectrum). Their 90 cm cavity had a τ_0 value of roughly 4 μs, and the bandwidth of the dye laser was similar to the Doppler width of the water vapor overtones (0.03−0.04 cm^{-1}). Operation at lower absorption signal levels (≤5 Torr water vapor) and pressure-broadened conditions (~250 Torr N_2 buffer gas) avoided errors due to nonexponential ring-down transients. They directly compared CRDS to photoacoustic spectroscopy. Because they probed $H_2{}^{16}O$ and $H_2{}^{18}O$ lines that originated from different lower states, their results were quite sensitive to temperature (0.6% for a 1 K change). The two laser spectroscopic techniques were in excellent agreement for $\delta^{18}O$ value of a water sample (Standard Light Arctic Precipitation, SLAP) relative to a standard, giving values of −55±7‰ from the CRDS measurement and −55±10‰ from the photoacoustic measurement. The value from mass spectrometric methods was −55.5‰. While the precision of the laser spectroscopic $\delta^{18}O$ measurements did not appear to equal that of the mass spectrometric determination, the accuracy of the former was good and, as the authors noted, the laser spectroscopic approached required a far smaller quantity of sample to perform the analysis.

6. Aerosol Extinction

Extinction by atmospheric aerosol is by far the clearest observable signal (above the constant Rayleigh background) in an HFCAS apparatus operating in ambient air in the UV, visible, or short wavelengths in the near-IR (at least to 1 μm). As early as 1988, Ramponi et al.,[11] in attempting to measure the water vapor absorption spectrum near 1.1 μm with a pulsed CRDS system, noted that the extinction from laboratory dust particles could dominate other loss processes. Romanini et al.[35] found an extinction signal present in their CW diode laser CRDS apparatus that reduced the ring-down time constant from 220 μs under vacuum to 60 μs in ambient, laboratory air, well beyond the extinction due to Rayleigh scattering. They suggested dust particles as the source. For researchers interested in measuring absorption due to homogeneous, gas-phase compounds, the aerosol extinction signal is simply a nuisance. A ring-down spectrometer is sensitive enough to detect single aerosol particles in a size range ≥0.3 μm[18] and the number of particles in this size range present in the small volume occupied by low-order transverse electric modes in an optical cavity can be small (≤1 cm^3). As a result, the aerosol extinction signal may exhibit gross fluctuations on successive ring-down transients that rapidly degrades sensitivity to homogeneous absorption. For example, in the absence of a particle filtration system on the inlet to our 662 nm NO_3 instrument, the sensitivity is typically at least 1 order of magnitude worse.[97] This "noise" or "background" due to aerosol extinction in CRDS comprises a signal that is important in its own right, however, for measurements of aerosol optical properties. Current techniques for characterization of aerosol optical properties include integrating nephelometers for measurement of total scattering and filter absorption measurements or photoacoustic spectroscopy for total absorption.[118] A sensitive, total extinction measurement would provide an excellent complement to currently available methods, and there is growing interest in the measurement of aerosol optical properties. Absorption and scattering by atmospheric aerosol affects regional visibility. It also influences the Earth's overall radiation budget and, therefore, its climate.[70]

The first study aimed at CRDS detection of particles was that of Sappey et al.[119] They used a pulsed CRDS apparatus at two different wavelengths (sequentially, not simultaneously), the second (532 nm) and third (355 nm) harmonics of a Nd:YAG laser. Their 98 cm, near confocal cavity had a τ_0 value of 107 μs in ambient air and a measurement precision of $\Delta\tau_{min} = 0.025$ μs, for a reported detection sensitivity better than 10^{-10} cm^{-1}. Due to the increase in Rayleigh scattering and the decrease in reflectivity of available mirrors in the UV, the instrument was at least an order of magnitude less sensitive at 355 nm. These authors compared the observed time constants obtained in ambient air that had passed through different types of filters to Mie scattering calculations based on the number and estimated size ranges of particles in the same air flow measured by two different particle counters. They concluded that the CRDS measurement was not particularly useful as a means of particle detection alone since the particle counters used in series with the CRDS instrument were far more sensitive. Vander Wal and Ticich[120] applied CRDS to the detection of soot particles in a flame for combustion research. They considered CRDS as a calibration for laser-induced incandescence (LII), a standard technique for measuring the soot volume fraction. Like the one described above, their apparatus included a 532 nm pulsed Nd:YAG and a 30 cm optical cavity comprised of two mirrors of $R = 99.7\%$. Although the resulting τ_0 value was well under 1 μs, the sensitivity of the apparatus was easily sufficient for a robust comparison with LII. The CRDS and LII methods gave quite similar results for absorbance measurements in different methane−air flames.

Smith and Atkinson[121] were the first to demonstrate direct measurement of extinction due to aerosol in ambient air. Their portable, pulsed CRDS instrument was also based on the conveniently available harmonics of a Nd:YAG laser. A 30 Hz Nd:YAG laser produced 1064 and 532 nm, that entered the same cavity, comprised of the same set of mirrors, simultaneously and collinearly. The two wavelengths were dispersed at the cavity output and detected separately. The near-confocal cavity was 96 cm in length. The mirrors were coated for simultaneous, maximum reflectivity at both wavelengths. The τ_0 value at both 532 and 1064 nm was roughly 5 μs, and the sensitivity was 10^{-8} cm^{-1} for a 5 s integra-

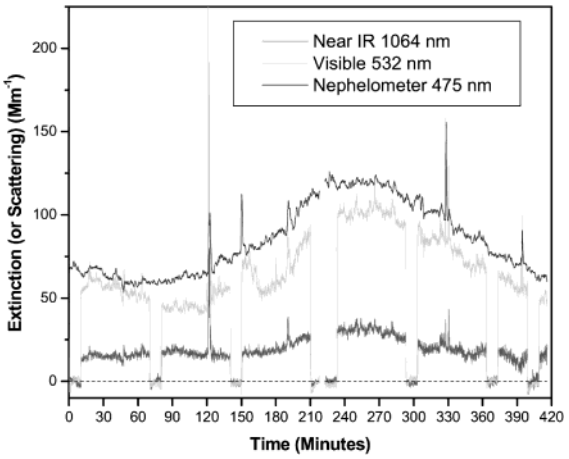

Figure 8. Time series of pulsed CRDS measurements in ambient air in the Portland, OR, area. The CRDS data are at two wavelengths, 1064 (lower trace) and 532 (middle trace) nm, and show the extinction signal due to aerosol. The data are influenced by wildfires in the Columbia River Gorge area, and the extinction spikes are due to smokers who occasionally approached the instrument inlet. For comparison, nephelometer data at 475 nm (upper trace) is also shown. (Reprinted with permission from ref 122.)

tion. Testing of the instrument by sampling ambient air from the Portland, OR, area on two separate days with variable air quality demonstrated the feasibility of the measurement. The inlet system, which entered the cavity from the center and exited to the pumps through ports adjacent to each of the end mirrors, was equipped with impact filters for size selection of ambient aerosol. They obtained a zero measurement by passing air samples through a dryer and an aerosol filter. There was no calibration of the air samples with other instrumentation, so quantitative assessment of instrument performance was not possible. Figure 8 shows recent, unpublished data from these authors[122] that illustrates aerosol extinction measurements at 532 and 1064 nm from air sampled in the Portland, OR, area.

Thompson et al.[123,124] also presented a proof of concept measurement for CRDS measurements of aerosol extinction. Their instrument was based on a high repetition rate (10 kHz) pulsed Cu vapor laser operating at 510 and 578 nm. Their 1.7 m cavity had τ_0 values near 8 μs at both wavelengths. The quoted sensitivity was 10^{-8} cm^{-1} (3σ) in a 1500 (0.15 s) laser shot average, although the temporal response of the air sampling system was limited to 30 s. These authors sampled ambient air (Gainesville, FL) from a laboratory window through a 6 m duct over a two month period. The sampling system was necessary because the prototype system was not portable. Zero measurements came from passing the same air flow through an efficient particle filter. They calibrated their instrument by measuring Rayleigh scattering cross sections in five different gases (N_2, O_2, Ar, CO_2, and SF_6) and by dual-wavelength measurement of extinction due to ~0.4 μm NaCl particles generated from a laboratory source. The ratio of extinction measurements at the two wavelengths were close to the value anticipated from Mie scattering calculations. Their ambient air demonstrations showed increases in aerosol extinction attributable to a local wildfire and to a fireworks demonstration. Finally, using an inertial impact filter system, these authors recorded a size-resolved extinction spectrum of ambient air, similar to that of Smith and Atkinson[121] described above.

Bulatov et al.[125] used a pulsed dye laser at 620 nm to pump a 75 cm cavity with $R = 99.95\%$ mirrors. The system had a τ_0 value of 1.7 μs and a sensitivity of $\alpha_{min} = 8 \times 10^{-8}$ cm^{-1} for a 128 laser shot average. They observed aerosol extinction signals in laboratory air and from prepared samples of NaCl and $CuCl_2 \cdot 2H_2O$ aerosol. For the latter samples, they used a solution atomizer that was capable of producing monodisperse aerosol of known size (over a range 0.2−2 μm) and number density (measured using a commercial process aerosol monitor). The salt aerosol flow crossed the ring-down cavity perpendicular to its axis. Measured extinction vs aerosol size agreed well with Mie scattering calculations for NaCl but not for $CuCl_2 \cdot 2H_2O$, which forms an orthorhombic crystal shape. This study is the first to demonstrate quantitative agreement of an experimental ring-down aerosol extinction measurement and that calculated from a well-characterized aerosol sample.

Strawa et al.[126] produced a prototype aerosol CRDS extinction measurement based on CW laser sources at two wavelengths, 690 and 1550 nm. Both wavelengths propagated simultaneously through the same three-mirror cavity (a narrow, isosceles triangle) with a total path length of 36 cm in the sample volume. The optical layout of the instrument had a small footprint and was designed for aircraft deployment. They recorded ring-down transients (time constants on the order of microseconds) using a cavity piezoelectric sweep at a repetition rate of 50−100 Hz to achieve a sensitivity of $\alpha_{min} = 1.5 \times 10^{-8}$ cm^{-1} for a 10 s average. This instrument is unique in that it incorporates a simultaneous scattering measurement via a glass wall on the flow system for direct measurement of single-scattering albedo (ratio of scattering to extinction). They measured extinction from samples of ammonium sulfate and polystyrene spheres in the laboratory, although they could not accurately assess the extinction measurement in comparison to Mie scattering theory because of uncertainties in characterization of particle number density and size distribution. They also field tested the instrument at a ground site at NASA Ames research center. Although they found some difficulty with mirror reflectivity degradation under high-aerosol loading, they observed extinction and scattering in ambient air, finding albedo values in the range 0.75 to ~1 depending on the air sample.

Finally, Pettersson et al.[127] measured aerosol extinction at 532 nm using a pulsed Nd:YAG laser. The lab-based measurements are to serve as a the basis for construction of a field instrument. They demonstrated quantitative agreement between Mie scattering theory and measured extinction in samples of polystyrene spheres over a range of particle number densities and sizes.

These examples of aerosol extinction measurements using cavity ring-down demonstrate that the technique is well suited to this purpose. Aerosol

extinction is broad-band, strongest at shorter wavelengths (i.e., UV and visible), and does not require particularly high sensitivity to observe in the lower atmosphere; therefore, the problem is amenable to measurement via the experimentally simple pulsed CRDS approach, although CW-based systems may carry a number of the advantages discussed above, such as lower power consumption, size, and weight. Portable and laboratory-based CRDS instruments will likely prove invaluable in the future for the measurement of visibility, air quality, and the impact of aerosol emissions on climate.

7. Conclusion

Cavity ring-down spectroscopy (CRDS) and its companion techniques, cavity-enhanced absorption spectroscopy (CEA) and integrated cavity output spectroscopy (ICOS), are promising, if as yet largely untested, methods for atmospheric trace gas analysis. They derive high sensitivity for direct absorption measurements from the long optical paths inside of high-finesse cavities. As field instruments, they may provide compact, low power, and potentially low-cost instrumentation that deliver high sensitivity, rapid time-response, and in situ sampling. As the discussion above has outlined, the method is sufficiently general to be applicable to a wide variety of atmospherically relevant compounds, including organic compounds, ammonia, nitrogen oxides, hydroxyl radicals, and elemental mercury. The approach is also valid for isotope ratio measurements and characterization of the optical properties of ambient aerosol. Indeed, there are more potential applications than the preceding examples have illustrated. The generality arises from breadth of the spectral coverage, from the far UV to the mid-IR. Although the number of published results from actual field instruments based on these methods remains small, more are sure to come. The fact that many examples of CRDS-based atmospheric trace gas detectors and aerosol extinction measurements at the time of this writing are in the proof of concept stage should make the next few years very interesting indeed.

8. Acknowledgments

The author thanks Harald Stark, Mattias Aldener, Anders Petterson, and Richard Fox for useful discussions. Thanks also to Erik Richard, Joost de Gouw, Eric Williams, John Nowak, Tom Ryerson, and Chuck Brock for providing supplemental information on atmospheric trace gas detection and aerosol properties. This work was funded in part by NOAA's Climate and Global Change Program.

9. References

(1) *Air Monitoring by Spectroscopic Techniques*; Sigrist, M. W., Ed.; John Wiley & Sons: New York, 1994; Vol. 127.
(2) *Spectroscopy in Environmental Science*; Clark, R. J. H., Hester, R. E., Eds.; John Wiley & Sons: Chichester, 1995; Vol. 24.
(3) O'Keefe, A.; Deacon, D. A. G. *Rev. Sci. Instrum.* **1988**, *59*, 2544.
(4) *Cavity-Ringdown Spectroscopy*; Busch, K. W., Busch, M. A., Eds.; American Chemical Society: Washington, DC, 1999.
(5) Scherer, J. J.; Paul, J. B.; O'Keefe, A.; Saykally, R. J. *Chem. Rev.* **1997**, *97*, 25.
(6) Wheeler, M. D.; Newman, S. M.; Orr-Ewing, A. J.; Ashfold, M. N. R. *J. Chem. Soc., Faraday Trans.* **1998**, *94*, 337.
(7) Berden, G.; Peeters, R.; Meijer, G. *Int. Rev. Phys. Chem.* **2000**, *19*, 565.
(8) Engeln, R.; Berden, G.; Peeters, R.; Meijer, G. *Rev. Sci. Instrum.* **1998**, *69*, 3763.
(9) O'Keefe, A. *Chem. Phys. Lett.* **1998**, *293*, 331.
(10) O'Keefe, A.; Scherer, J. J.; Paul, J. B. *Chem. Phys. Lett.* **1999**, *307*, 343.
(11) Ramponi, A. J.; Milanovich, F. P.; Kan, T.; Deacon, D. *Appl. Opt.* **1988**, *27*, 4606.
(12) O'Keefe, A.; Lee, O. *Am. Lab.* **1989**, *21*, 19.
(13) Berden, G.; Peeters, R.; Meijer, G. *Chem. Phys. Lett.* **1999**, *307*, 131.
(14) Jongma, R. T.; Boogarts, G. H. M.; Holleman, I.; Meijer, G. *Rev. Sci. Instrum.* **1995**, *66*, 2821.
(15) Vasudev, R.; Usachev, A.; Dunsford, W. R. *Environ. Sci. Technol.* **1999**, *33*, 1936.
(16) Mürtz, M.; Frech, B.; Urban, W. *Appl. Phys. B* **1999**, *68*, 243.
(17) Atkinson, D. B. *Analyst* **2003**, *128*, 117.
(18) Brown, S. S.; Stark, H.; Ravishankara, A. R. *Appl. Phys. B* **2002**, *75*, 173.
(19) Zalicki, P.; Zare, R. N. *J. Chem. Phys.* **1995**, *102*, 2708.
(20) Hodges, J. T.; Looney, J. P.; van Zee, R. D. *J. Chem. Phys.* **1996**, *105*, 10278.
(21) Lehmann, K. K.; Romanini, D. *J. Chem. Phys.* **1996**, *105*, 10.
(22) Naus, H.; van Stokkum, I. H. M.; Hogervorst, H.; Ubachs, W. *Appl. Opt.* **2001**, *40*, 4416.
(23) Spuler, S.; Linne, M. *Appl. Opt.* **2002**, *41*, 2858.
(24) Lee, D.-H.; Yoon, Y.; Kim, B.; Lee, J. Y.; Yoo, Y. S.; Hahn, J. W. *Appl. Phys. B.* **2002**, *74*, 435.
(25) Hodges, J. T.; Looney, J. P.; van Zee, R. D. *Appl. Opt.* **1996**, *35*, 4112.
(26) Newman, S. M.; Lane, I. C.; Orr-Ewing, A. J.; Newnham, D. A.; Ballard, J. *J. Chem. Phys.* **1999**, *110*, 10749.
(27) Yalin, A. P.; Zare, R. N. *Laser Phys.* **2002**, *12*, 1065.
(28) Brown, S. S.; Wilson, R. W.; Ravishankara, A. R. *J. Phys. Chem.* **2000**, *104*, 4976.
(29) Ball, S. M.; Povey, I. M.; Norton, E. G.; Jones, R. L. *Chem. Phys. Lett.* **2001**, *342*, 113.
(30) Scherer, J. J. *Chem. Phys. Lett.* **1998**, *292*, 143.
(31) Scherer, J. J.; Paul, J. B.; Jiao, H.; O'Keefe, A. *Appl. Opt.* **2001**, *40*, 6725.
(32) Czyzewski, A.; Chudzynski, S.; Ernst, K.; Karasinski, G.; Kilianek, L.; Pietruczuk, A.; Skubiszak, W.; Stacewicz, T.; Stelmaszcyk, K.; Koch, B.; Rairoux, P. *Opt. Commun.* **2001**, *191*, 271.
(33) Engeln, R.; Meijer *Rev. Sci. Instrum.* **1996**, *67*, 2708.
(34) Romanini, D.; Kachanov, A. A.; Sadeghi, N.; Stoeckel, F. *Chem. Phys. Lett.* **1997**, *264*, 316.
(35) Romanini, D.; Kachanov, A. A.; Stoeckel, F. *Chem. Phys. Lett.* **1997**, *270*, 538.
(36) Paldus, B. A.; Harris, J. S. J.; Martin, J.; Xie, J.; Zare, R. N. *J. Appl. Phys.* **1997**, *82*, 3199.
(37) He, Y.; Orr, B. J. *Chem. Phys. Lett.* **2000**, *319*, 131.
(38) Schulz, K. J.; Simpson, W. R. *Chem. Phys. Lett.* **1998**, *297*, 523.
(39) Paldus, B. A.; Harb, C. C.; Spence, T. G.; Wilke, B.; Xie, J.; Harris, J. S.; Zare, R. N. *J. Appl. Phys.* **1998**, *83*, 3991.
(40) Spence, T. G.; Harb, C. C.; Paldus, B. A.; Zare, R. N.; Willke, B.; Byer, R. L. *Rev. Sci. Instrum.* **2000**, *71*, 347.
(41) Levenson, M. D.; Paldus, B. A.; Spence, T. G.; Harb, C. C.; Harris, J. S. J.; Zare, R. N. *Chem. Phys. Lett.* **1998**, *290*, 335.
(42) Paul, J. B.; Lapson, L.; Anderson, J. G. *Appl. Opt.* **2001**, *40*, 4904.
(43) Baer, D. S.; Paul, J. B.; Gupta, M.; O'Keefe, A. O. *Appl. Phys. B* **2002**, *75*, 261.
(44) Kleine, D.; Mürtz, M.; Lauterbach, J.; Dainke, H.; Urban, W.; Hering, P.; Kleinermanns, K. *Israel J. Chem.* **2001**, *41*, 111.
(45) Gopalsami, N.; Raptis, A. C.; Meier, J. *Rev. Sci. Instrum.* **2002**, *73*, 259.
(46) Crim, F. F. *Annu. Rev. Phys. Chem.* **1984**, *35*, 657.
(47) Scherer, J. J.; Voelkel, D.; Rakestraw, D. J.; Paul, J. B.; Collier, C. P.; Saykally, R. J.; O'Keefe, A. *Chem. Phys. Lett.* **1995**, *245*, 273.
(48) Paldus, B. A.; Harb, C. C.; Spence, T. G.; Zare, R. N.; Gmachl, C.; Capasso, F.; Sivco, D. L.; Baillargeon, J. N.; Hutchinson, A. L.; Cho, A. Y. *Opt. Lett.* **2000**, *25*, 666.
(49) Kosterev, A. A.; Tittel, F. K. *IEEE J. Quantum Elec.* **2002**, *38*, 582.
(50) Dlugokencky, E. J.; Masarie, K. A.; Lang, P. M.; Tans, P. P. *Nature* **1998**, *393*, 447.
(51) Webster, C. R.; Flesch, G. J.; Scott, D. C.; Swanson, J.; May, R. D.; Woodward, W. S.; Gmachl, C.; Capasso, F.; Sivico, D. L.; Baillargeon, J. N.; Hutchinson, A. L.; Cho, A. Y. *Appl. Opt.* **2001**, *40*, 321.
(52) Richard, E. C.; Kelly, K. K.; Winkler, R. H.; Wilson, R.; Thompson, R. L.; McLaughlin, R. J.; Schmeltekopf, A. L.; Tuck, A. F. *Appl. Phys. B.* **2002**, *75*, 183.
(53) Fawcett, B. L.; Parkes, A. M.; Shallcross, D. E.; Orr-Ewing, A. J. *Phys. Chem. Chem. Phys.* **2002**, *4*, 5960.

(54) Barry, H. R.; Corner, L.; Hancock, G.; Peverall, R.; Ritchie, G. A. D. *Chem. Phys. Lett.* **2001**, *333*, 285.
(55) Cao, X.-L.; Hewitt, N. In *Reactive Hydrocarbons in the Atmosphere*; Hewitt, N., Ed.; Academic Press: San Diego, 1999.
(56) Lindiger, W.; Hansel, A.; Jordan, A. *Int. J. Mass. Spectrom. Ion Processes* **1998**, *173*, 191.
(57) Dahnke, H.; Kleine, D.; Hering, P.; Mürtz, M. *Appl. Phys. B* **2001**, *72*, 971.
(58) Bucher, C. R.; Lehmann, K. K.; Plusquellic, D. F.; Fraser, G. T. *Appl. Opt.* **2000**, *39*, 3154.
(59) Peeters, R.; Berden, G.; Alafsson, A.; Laarhoven, L. J. J.; Meijer, G. *Chem. Phys. Lett.* **2001**, *337*, 231.
(60) Parkes, A. M.; Fawcett, B. L.; Austin, R. E.; Nakamichi, S.; Shallcross, D. E.; Orr-Ewing, A. J. *Analyst* **2003**, *128*, 960.
(61) Awtry, A. R.; Miller, J. H. *Appl. Phys. B* **2002**, *75*, 255.
(62) Todd, M. W.; Provencal, R. A.; Owano, T. G.; Paldus, B. A.; Kachanov, A.; Vodopyanov, K. L.; Hunter, M.; Coy, S. L.; Steinfeld, J. I.; Arnold, J. T. *Appl. Phys. B* **2002**, *75*, 367.
(63) Finlayson-Pitts, B. J.; Pitts, J. N. J. *Chemistry of the Upper and Lower Atmosphere*; Academic Press: San Diego, CA, 2000.
(64) Platt, U. In *Air Monitoring by Spectroscopic Techniques*; Sigrist, M. W., Ed.; John Wiley & Sons: New York, 1994.
(65) Plane, J. M. C.; Smith, N. In *Spectroscopy in Environmental Science*; Clark, R. J. H., Hester, R. E., Eds.; John Wiley & Sons: Chichester, 1995.
(66) Fried, A.; Henry, B.; Wert, B.; Sewell, S.; Drummond, J. R. *Appl. Phys. B* **1998**, *67*, 317.
(67) Kormann, R.; Fischer, H.; Gurk, C.; Helleis, R.; Klüpfel, T.; Kowalski, K.; Königstedt, R.; Parchatka, U.; Wagner, V. *Spectrochim. Acta, Part A* **2002**, *58*, 2488.
(68) Barry, H.; Corner, L.; Hancock, G.; Peverall, R.; Ritchie, G. A. D. *Phys. Chem. Chem. Phys.* **2002**, *4*, 445.
(69) Dahnke, H.; Von Basum, G.; Kleinermanns, K.; Hering, P.; Mürtz, M. *Appl. Phys. B* **2002**, *75*, 311.
(70) *Climate Change 2001: The Scientific Basis*; Houghton, J. T., Ding, Y., Griggs, D. J., Noguer, M., van der Linden, P. J., Dai, X., Maskell, K., Johnson, C. A., Eds.; Cambridge University Press: Cambridge, 2001.
(71) Conway, T. J.; Tans, P. P.; Waterman, L. S.; Thoning, K. W.; Kitzis, D. R.; Masarie, K. A.; Zhang, N. *J. Geophys. Res.* **1994**, *99*, 22.
(72) Parrish, D. D.; Holloway, J. S.; Fehsenfeld, F. C. *Environ. Sci. Technol.* **1994**, *28*, 1615.
(73) Fried, A.; Henry, B.; Parrish, D. D.; Carpenter, J. R.; Buhr, M. P. *Atmos. Environ.* **1991**, *25A*, 2277.
(74) He, Y.; Orr, B. J. *Appl. Phys. B* **2002**, *75*, 267.
(75) Fehsenfeld, F. C.; Huey, L. G.; Leibrock, E.; Dissly, R.; Williams, E.; Ryerson, T. B.; Norton, R.; Sueper, D. T.; Hartsell, B. *J. Geophys. Res.* **2002**, *107*, doi: 10.1029/2001JD001327.
(76) Claps, R.; Englich, R. V.; Leleux, D. P.; Richter, D.; Tittel, F. K.; Curl, R. F. *Appl. Opt.* **2001**, *40*, 4387.
(77) Williams, E. J.; Sandholm, S. T.; Bradshaw, J. D.; Schendel, J. S.; Langford, A. O.; Quinn, P. K.; LeBel, P. J.; Vay, S. A.; Roberts, P. D.; Norton, R. B.; Watkins, B. A.; Buhr, M. P.; Parrish, D. D.; Calvert, J. G.; Fehsenfeld, F. C. *J. Geophys. Res.* **1992**, *97*, 11.
(78) Owens, M. A.; Davis, C. C.; Dickerson, R. R. *Anal. Chem.* **1999**, *71*, 1391.
(79) Pakkan, T. A.; Hillamo, R. E.; Aurela, M.; Andersen, H. V.; Grundahl, L.; Ferm, M.; Persson, K.; Karlsson, V.; Reissell, A.; Røyset, O.; Fløisand, I.; Oyola, P.; Ganko, T. *J. Aerosol Sci.* **1999**, *30*, 247.
(80) Peeters, R.; Berden, G.; Apituley, A.; Meijer, G. *Appl. Phys. B* **2000**, *71*, 231.
(81) Fontjin, A.; Sabadell, A. J.; Ronco, R. J. *Anal. Chem.* **1970**, *42*, 575.
(82) Ryerson, T. B.; Williams, E. J.; Fehsenfeld, F. C. *J. Geophys. Res.* **2000**, *105*, 26447.
(83) Thornton, J. A.; Wooldrige, P. J.; Cohen, R. J. *Anal. Chem.* **2000**, *72*, 528.
(84) Menzel, L.; Kosterev, A. A.; Curl, R. F.; Tittel, F. K.; Gmachl, C.; Capasso, F.; Sivco, D. L.; Baillargeon, J. N.; Hutchinson, A. L.; Cho, A. Y.; Urban, W. *Appl. Phys. B* **2001**, *72*, 859.
(85) O'Keefe, A.; Scherer, J. J.; Paul, J. B.; Saykally, R. J. In *Cavity-Ringdown Spectroscopy*; Busch, K. W., Busch, M. A., Eds.; American Chemical Society: Washington, DC, 1999.
(86) Lauterbach, J.; Kleine, D.; Kleinermanns, K.; Hering, P. *Appl. Phys. B* **2000**, *71*, 873.
(87) Evertsen, R.; Staicu, A.; Dam, N.; Van Vliet, A.; Ter meulen, J. J. *Appl. Phys. B* **2002**, *74*, 465.
(88) Mazurenka, M. I.; Fawcett, B. L.; Elks, J. M. F.; Shallcross, D. E.; Orr-Ewing, A. J. *Chem. Phys. Lett.* **2003**, *367*, 1.
(89) Kasyutich, V. L.; Bale, C. S. E.; Canosa-Mas, C. E.; Pfrang, C.; Vaughan, S.; Wayne, R. P. *Appl. Phys. B* **2003**, *76*, 691.
(90) Noxon, J. F.; Norton, R. B.; Henderson, W. R. *Geophys. Res. Lett.* **1978**, *5*, 675.
(91) Platt, U.; Perner, D. *Geophys. Res. Lett.* **1980**, *7*, 89.
(92) Toon, G. C.; Farmer, C. B.; Norton, R. H. *Nature* **1986**, *319*, 570.
(93) King, M. D.; Dick, E. M.; Simpson, W. R. *Atmos. Environ.* **2000**, *34*, 685.
(94) Yokelson, R. J.; Burkholder, J. B.; Fox, R. W.; Talukdar, R. K.; Ravishankara, A. R. *J. Phys. Chem.* **1994**, *98*, 13144
(95) Simpson, W. R. *Rev. Sci. Instrum.* **2003**, *74*, 3442.
(96) Brown, S. S.; Stark, H.; Ciciora, S. J.; Ravishankara, A. R. *Geophys. Res. Lett.* **2001**, *28*, 3227.
(97) Brown, S. S.; Stark, H.; Ciciora, S. J.; McLaughlin, R. J.; Ravishankara, A. R. *Rev. Sci. Instrum.* **2002**, *73*, 3291.
(98) Brown, S. S.; Stark, H.; Ryerson, T. B.; Williams, E. J.; Nicks, D. K. J.; Trainer, M.; Fehsenfeld, F. C.; Ravishankara, A. R. *J. Geophys. Res.* **2003**, *108*, doi: 10.1029/2002JD002917.
(99) Brown, S. S.; Stark, H.; Aldener, M.; Ravishankara *J. Geophys. Res.* Manuscript in preparation.
(100) Kasyutich, V. L.; Canosa-Mas, C. E.; Pfrang, C.; Vaughan, S.; Wayne, R. P. *Appl. Phys. B* **2002**, *75*, 755.
(101) Finlayson-Pitts, B. J.; Wingen, L. M.; Sumner, A. L.; Syomin, D.; Ramazan, K. A. *Phys. Chem. Chem. Phys.* **2003**, *5*, 223.
(102) Wang, L.; Zhang, J. *Environ. Sci. Technol.* **2000**, *34*, 4221.
(103) Crosley, D. R. *J. Atmos. Sci.* **1995**, *52*, 3299.
(104) Mount, G. H. *J. Geophys. Res.* **1992**, *97*, 2427.
(105) Creasey, D. J.; HalfordMaw, P. A.; Heard, D. E.; Pilling, M. J.; Whitaker, B. J. *J. Chem. Soc., Faraday Trans.* **1997**, *93*, 2907.
(106) Mather, J. H.; Stevens, P. S.; Brune, W. H. *J. Geophys. Res.* **1997**, *102*, 6427.
(107) Tanner, D. J.; Jefferson, A.; Eisele, F. L. *J. Geophys. Res.* **1997**, *102*, 6415.
(108) Spaanjaars, J. J. L.; ter Meulen, J. J.; Meijer, G. *J. Chem. Phys.* **1997**, *107*, 2242.
(109) Peeters, R.; Berden, G.; Meijer, G. *Appl. Phys. B* **2001**, *73*, 65.
(110) Barry, H. R.; Bakowski, B.; Corner, L.; Freegarde, T.; Hawkins, O. T. W.; Hancock, G.; Jacobs, R. M. J.; Peverall, R.; Ritchie, G. A. D. *Chem. Phys. Lett.* **2000**, *319*, 125.
(111) Spuler, S.; Linne, M.; Sappey, A.; Snyder, S. *Appl. Opt.* **2000**, *39*, 2480.
(112) Tao, S.; Mazzotti, F. J.; Winstead, C. B.; Miller, G. P. *Analyst* **2000**, *125*, 1021.
(113) Miller, J. B.; Mack, K. A.; Dissly, R.; White, J. W. C.; Dlugokencky, E. J.; Tans, P. P. *J. Geophys. Res.* **2002**, *107*, doi: 10.1029/2001JD000630.
(114) Kleine, D.; Dahnke, H.; Urban, W.; Hering, P.; Mürtz, M. *Opt. Lett.* **2000**, *25*, 1606.
(115) Dahnke, H.; Kleine, D.; Urban, W.; Hering, P.; Mürtz, M. *Appl. Phys. B* **2001**, *72*, 121.
(116) Crosson, E. R.; Ricci, K. N.; Richman, B. A.; Chilese, F. C.; Owano, T. G.; Provencal, R. A.; Todd, M. W.; Glasser, J.; Kachanov, A. A.; Paldus, B. A.; Spence, T. G.; Zare, R. N. *Anal. Chem.* **2002**, *74*, 2003.
(117) Samura, K.; Hashimoto, S. H.; Kawasaki, M.; Hayashida, A.; Kagi, E.; Ishiwata, T.; Matsumi, Y. *Appl. Opt.* **2002**, *41*, 2349.
(118) McMurry, P. H. *Atmos. Environ.* **2000**, *34*, 1959.
(119) Sappey, A. D.; Hill, E. S.; Settersten, T.; Linne, M. A. *Opt. Lett.* **1998**, *23*, 954.
(120) Vander Wal, R. L.; Ticich, T. M. *Appl. Opt.* **1999**, *38*, 1444.
(121) Smith, J.; Atkinson, D. B. *Analyst* **2001**, *126*, 1216.
(122) Atkinson, D. B. Personal communication.
(123) Thompson, J. E.; Smith, B. W.; Winefordner, J. D. *Anal. Chem.* **2002**, *74*, 1962.
(124) Thompson, J. E.; Nasajpour, H. D.; Smith, B. W.; Winefordner, J. D. *Aerosol Sci. Technol.* **2003**, *37*, 221.
(125) Bulatov, V.; Fisher, M.; Schechter, I. *Anal. Chim. Acta* **2002**, *466*, 1.
(126) Strawa, A. W.; Casteneda, R.; Owano, T.; Baer, D. S.; Paldus, B. A. *J. Atmos. Oceanic Technol.* **2003**, *20*, 454.
(127) Pettersson, A.; Lovejoy, E.; Brown, S. S.; Brock, C.; Ravishankara, A. R. *J. Aerosol Sci.* Manuscrpt in preparation.

CR020645C